The Fluid Mechanics Inside a Volcano

Helge M. Gonnermann[1] and Michael Manga[2]

[1]Department of Earth and Planetary Sciences, Harvard University, Cambridge, Massachussetts 02138; email: gonnermann@eps.harvard.edu

[2]Department of Earth and Planetary Science, University of California, Berkeley, California 94720-4767; email: manga@seismo.berkeley.edu

Annu. Rev. Fluid Mech. 2007. 39:321–56

The *Annual Review of Fluid Mechanics* is online at fluid.annualreviews.org

This article's doi:
10.1146/annurev.fluid.39.050905.110207

0066-4189/07/0115-0321$20.00

Key Words

bubble nucleation, bubble growth, fragmentation, volcanic eruption, magma rheology

Abstract

The style and evolution of volcanic eruptions are dictated by the fluid mechanics governing magma ascent. Decompression during ascent causes dissolved volatile species, such as water and carbon dioxide, to exsolve from the melt to form bubbles, thus providing a driving force for the eruption. Ascent is influenced not only by the nucleation and growth of gas bubbles, but also magma rheology and brittle deformation (fragmentation). In fact, all processes and magma properties within the conduit interact and are coupled. Ultimately, it is the ability of gas trapped within growing bubbles to expand or to be lost by permeable gas flow, which determines whether ascending magmas can erupt nonexplosively. We review and integrate models of the primary conduit processes to show when each process or property dominates and how these interact within a conduit. In particular, we illustrate how and why ascent rate may control eruptive behavior: slowly ascending magmas erupt effusively and rapidly ascending magmas erupt explosively.

1. INTRODUCTION

Explosive eruption: eruption in which the magma travels through the atmosphere in the form of discrete pieces

Volcanoes display a wide range of eruption styles, from the effusion of lava flows or domes over periods of days to decades, to explosive eruptions that may last for as little as seconds or that may be sustained over many days and eject material into the stratosphere.

In part, the difference in eruption style can be associated with different magma viscosities: Low-viscosity, $O(1 - 10^3)$ Pa s, magmas tend to erupt effusively, whereas more viscous magmas, $> O(10^6)$ Pa s, tend to erupt explosively. A given volcano, however, can erupt the same magmas in the full range of eruption styles, e.g., Mayor Island in New Zealand (Houghton et al. 1992). The style of volcanic eruption is thus not solely governed by magma viscosity.

Understanding the processes that result in different eruption styles is a central theme in physical volcanology. Why are there transitions in eruption style? Is there a pattern in eruption style? What features of erupted materials diagnose processes that occur within the volcanic conduit through which magma rises from the subsurface where it is stored and accumulates? The answers to these questions lie in part in understanding the feedback between the various fluid mechanics processes that operate within the conduit.

Here we review the key processes that occur as magma rises to the surface within a conduit, and use numerical simulations of these processes to illustrate some of the interactions. We focus on magmatic eruptions (molten rock), but note that the ideas and processes are relevant to eruptions in general, including geysers, mud volcanoes, and cryovolcanoes that erupt melted ice.

2. HOW DO VOLCANOS WORK?

Figure 1 is a schematic illustration of a volcano. Magma, stored in a magma chamber, contains dissolved volatile species, primarily water. Carbon dioxide and sulphur dioxide are usually present in smaller amounts, but are important both for eruption dynamics and the effects of eruptions on climate. Magma within the magma chamber may already be supersaturated in volatiles and contain a pre-eruptive exsolved gas phase (Wallace et al. 1995), or it may become supersaturated upon ascent-driven decompression, causing bubbles to nucleate at the exsolution depth and to grow as the magma continues to rise. The growth of bubbles causes the rising magma to accelerate, assuming conduit width does not change. At some point, the magma may fragment into discrete pieces. These fragments make up the material that erupts explosively in eruption columns; if magma reaches the surface without fragmenting, the eruption is termed effusive and forms lava flows (**http://www.volcano.si.edu/world/tpgallery.cfm**).

Eruptions can be initiated in numerous ways. Magma can be driven to the surface by overpressure within the magma chamber (Blake 1984, Jellinek & DePaolo 2003, McLeod & Tait 1999). Pressure in a magma chamber can increase if fresh magma is injected, or if bubbles form as the magma cools and crystallizes (Wallace 2001). Eruptions can also be triggered from above if a large surface load is removed, e.g.,

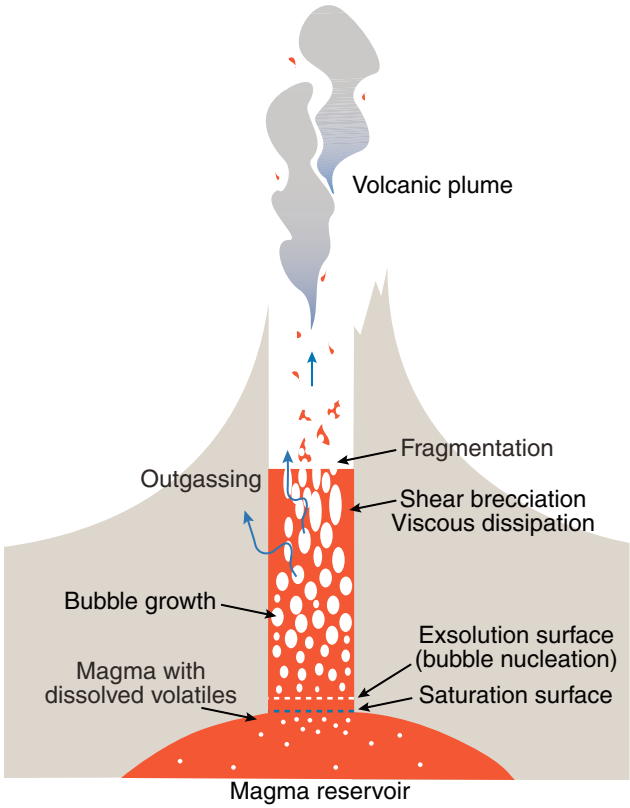

Figure 1

Schematic illustration of a volcano. Magma contains dissolved volatiles (predominantly water, CO_2, SO_2). Upon ascent-driven decompression, volatile solubility decreases and magma becomes supersaturated in volatiles. Gas bubbles nucleate at the exsolution surface. Volatiles continue to exsolve and bubbles grow during magma ascent above the exsolution surface. Gas may be lost from the magma by permeable gas flow through porous and/or fractured magma. Gas may escape radially into conduit walls or vertically through the magma column to the atmosphere. During explosive eruptions, bubble walls rupture catastrophically at the fragmentation surface. The released gas expands rapidly and magma ascent changes from a viscous melt with suspended bubbles to a gas flow with suspended magma fragments.

by a landslide, which allows stored magma to decompress (Lipman & Mullineaux 1981).

One important fluid mechanical process we do not discuss beyond this section is the interaction of magma in the conduit with externally derived water (as opposed to water dissolved in the magma, which forms bubbles), either groundwater or water stored in lakes or the ocean. Eruptions influenced by external water are usually termed phreatomagmatic eruptions and are not uncommon. In fact, Schmincke (2004) writes "there is hardly a volcanic eruption that has not been influenced in some ways by magma-water contact." If heat exchange from hot magma to water occurs fast enough,

Phreatomagmatic eruption: eruption resulting from the interaction of magma and water initially stored external to the magma

the conversion of water to steam generates large pressures. Resulting eruptions tend to be very explosive because of the high ratio of thermal expansion to compressibility of water (Wohletz 1983). The ability of water to physically mix with the magma is important in order to have a large surface area for rapid heat transfer. Given the large differences in viscosity and density between water and magma, porous magma or already fragmented magma may be essential to enhance water-magma mixing and explosive eruption (Trigila et al. 2006), or a feedback between fragmentation and mixing may be important (Büttner & Zimanowski 1998).

Fragmentation: a process in which the magma transforms from a continuous melt phase with bubbles to discrete pieces of magma surrounded by a continuous gas phase

Effusive eruption: nonexplosive extrusion of magma to the surface to form lava flows and domes

It is important to note that not all magmas are created equal: Differences in composition of the melt affect its viscosity, which can vary from 1 Pa s (carbonatites) to $O(10^2)$ Pa s (basalts) to $>O(10^9)$ Pa s (rhyolites). Crystals, present in most magmas, also influence magma rheology. Furthermore, the tectonic setting where magmas are generated influences magma composition, volatile content, the rate at which magma is supplied to the magma chamber, and the overpressure needed for eruption. Hence, the great diversity in eruption style cannot be explained solely by fluid mechanics.

To a large extent, it is within the conduit where the dynamics of the eruption is determined and thus we focus on processes within the conduit. There is also a rich range of fluid mechanical processes below the conduit in magma chambers (Sparks et al. 1984), as well as above the conduit in lava flows for effusive eruptions (Griffiths 2000), and volcanic plumes and particulate density currents for explosive eruptions (Woods 1995).

3. FLUID MECHANICS

Bubbles are critical because they provide the driving force for eruptions, either by increasing buoyancy or by increasing magma chamber overpressure. The resulting ascent of the magma is governed by its rheology, as is the fragmentation process, and the ability of gases to separate from the magma. Hence, the life cycle of bubbles in magma controls, but also reflects, the eruption dynamics.

3.1. Birth: Bubble Nucleation

The volatile content of silicate melts depends strongly on pressure and to a lesser extent on temperature. Most melts are thought to be saturated in volatiles prior to eruption (Johnson et al. 1994, Wallace et al. 1995, Westrich 1992). As a consequence of magma differentiation and volatile saturated crystallization in magma storage regions, many magmas may also contain a pre-eruptive exsolved gas phase (Wallace 2004). Volatile solubility decreases with decreasing pressure and, hence, volatiles exsolve during ascent-driven decompression. At a given pressure and temperature, solubility depends on the composition of the coexisting gas phase. Models of volatile content of magmas are typically based on empirical formulations calibrated to equilibrium solubility experiments. Experimental measurements for silicic magmas are generally consistent with Henry's law, which predicts a square-root dependence of solubility on pressure (Blank et al. 1993). However, at pressures greater than about 50 megaPascals (MPa), volcanologically significant deviations occur (Liu et al. 2005, Papale 1999a).

Bubble nucleation can be heterogeneous or homogeneous (Gardner & Denis 2004, Mangan & Sisson 2000, Mourtada-Bonnefoi & Laporte 2004, Toramaru 1989) and requires a supersaturation pressure Δp_s to overcome the energy barrier provided by surface tension. Here Δp_s is defined as the difference between the hypothetical pressure at which dissolved volatiles would be in equilibrium with the melt and the ambient pressure p_m. Supersaturation can be achieved if diffusion of volatiles from the melt into the bubbles can not keep pace with the decrease in volatile solubility caused by ascent-driven decompression. In other words, the Peclet number for volatile exsolution $\mathrm{Pe}_{dif} = \tau_{dif}/\tau_{dec} \gg 1$ (Lensky et al. 2004, Navon et al. 1998, Toramaru 1995). Here $\tau_{dec} = p_m/\dot{p}_m$ is the characteristic decompression time, $\tau_{dif} = (S-R)^2/D$ is the characteristic time for volatile diffusion, R is bubble radius, S is the radial distance from bubble center to the midpoint between adjacent bubbles, D is volatile diffusivity in the melt, p_m is ambient pressure of the melt, and $\dot{p}_m$ is the decompression rate. As discussed in Section 3.3, high rates of bubble nucleation may result in the catastrophic overpressurization and volume expansion thought to be associated with explosive magma fragmentation.

Mafic: magma relatively poor in silica and rich in iron and magnesium

Classical nucleation theory (Hirth et al. 1970) predicts a very strong dependence of the homogeneous bubble nucleation rate $\mathcal{J}$ (number of bubbles per unit volume per unit time) on the supersaturation pressure Δp_s,

$$\mathcal{J} \propto \exp\left[-\frac{16\pi\gamma^3}{3kT\Delta P_s^2}\right], \quad (1)$$

where γ is surface tension, k is the Boltzmann constant, and T is temperature. Surface tension is typically between approximately 0.05 and 0.15 N/m, with a dependence on both temperature and composition of the melt (Mangan & Sisson 2005).

The critical supersaturation pressure $\Delta P_{s_{crit}}$ needed to trigger bubble nucleation during decompression can be determined experimentally by decreasing pressure of volatile-saturated magmas at a controlled rate. The barrier for homogeneous nucleation in crystal-free rhyolite is large, $\Delta P_{s_{crit}} > 100$ MPa, but much smaller in more mafic magmas (Mangan & Sisson 2000, Mourtada-Bonnefoi & Laporte 2004). Heterogeneous nucleation, in which the presence of certain crystals (e.g., Fe-Ti oxides) provides nucleation substrates because they lower surface tension, can greatly reduce $\Delta P_{s_{crit}}$ to less than a few megaPascals (Gardner & Denis 2004, Hurwitz & Navon 1994). Increases in water content and concentration of mafic crystals both reduce $\Delta P_{s_{crit}}$ (Mangan & Sisson 2005). The importance of large $\Delta P_{s_{crit}}$ for ascending, supersaturated magmas is that once bubbles do form they grow rapidly because of large gradients in volatile content. Rapid increases in vesicularity promote explosive eruption.

3.2. Life: Bubble Growth

Once bubbles nucleate, ascent-driven decompression continues to decrease volatile solubility, causing volatile diffusion from the melt to the melt-vapor interface. Volatile exsolution and expansion are impeded by surface tension and viscous stresses in the melt. Because surface tension forces are comparatively small (Sparks 1978), there are

three potentially rate-limiting processes during bubble growth: (*a*) the diffusion of volatiles to the melt-vapor interface, (*b*) the viscous flow of the melt, and (*c*) the rate of change in solubility caused by decompression.

Pyroclasts: fragments of magma ejected during eruption

3.2.1. Viscous limit. In the viscous limit ($\mathrm{Pe}_{vis} = \tau_{vis}/\tau_{dec} \gg 1$) surface tension, inertia, and diffusion can be neglected and bubble growth follows an exponential growth law (Lensky et al. 2004)

$$\hat{R} = \exp\left(\frac{\hat{t}^2}{2}\frac{\tau_{dec}}{\tau_{vis}}\right). \quad (2)$$

Here $\tau_{vis} = \eta_{melt}/\Delta p_m$ is the characteristic viscous timescale (Lensky et al. 2004, Navon et al. 1998, Toramaru 1995), τ_{dec} is the characteristic decompression timescale, η_{melt} is the melt viscosity, $\hat{R} = R/R_0$ is the nondimensional bubble radius, and $\hat{t} = t/\tau_{dec}$ is the nondimensional time. A subscript 0 throughout this paper refers to the initial value of the given variable. Viscous retardation of bubble growth is most significant at melt viscosities in excess of 10^9 Pa s, which generally corresponds to vesicularities in the range of 0.7 to 0.8 (Sparks et al. 1994, Toramaru 1995), shallow depths, and relatively low dissolved volatile contents. Here p_g, the gas pressure inside bubbles, can become significantly larger than p_m, resulting in the buildup of overpressure. Diffusion of volatiles to the melt-vapor interface is controlled by volatile solubility at that interface. Because the latter depends on p_g, viscosity-limited bubble growth leads to volatile supersaturation, a process sometimes referred to as "viscosity quench" (Thomas et al. 1994). In turn, gas overpressure and supersaturation increase the potential for subsequent accelerated bubble growth and/or rupture of the bubble wall (Section 3.3). Consequently, it has been proposed that lava domes can maintain high internal gas pressures on timescales comparable to their extrusion (Sato et al. 1992). Viscosity-limited bubble growth occurs in experiments at decompression rates of $>$ 0.1 MPa/s (Gardner et al. 2000), and is also predicted by numerical models of bubbles growth (Proussevitch & Sahagian 1998, Toramaru 1995) and **Figure 2*b***. It is also important for the expansion of pyroclasts during ascent above the fragmentation surface (Kaminski & Jaupart 1997).

Figure 2

Model simulations of diffusive bubble growth. Solid: constant decompression rate of $\dot{p}_m = 0.1$ megaPascals (MPa) s^{-1} and bubble number density, $N_d = 10^{11}$ m^{-3}. Long-dashed: $\dot{p}_m = 1$ MPa s^{-1} and bubble number density, $N_d = 10^{14}$ m^{-3}. Short-dashed: equilibrium model. Initial conditions are $\phi_0 = 0.001$, $c_{w,0} = 5$ wt.%, $c_{c,0} = 268$ ppm, $T_{g,0} = T_{m,0} = 850°$ C, and $p_{m,0} = 200$ MPa. (*a*) Note thinning of melt shell for the $\dot{p}_m = 0.1$ MPa s^{-1} case represented by scaled bubble cross sections and departure from equilibrium. (*b*) At $p_m < 20$ MPa viscosity increase results in $\mathrm{Pe}_{vis} \gg 1$ and in the case of $\dot{p}_m = 1$ MPa s^{-1} buildup of overpressure sufficient for fragmentation. (*c*, *d*) Supersaturation for $N_d = 10^{11}$ m^{-3} is larger than for $N_d = 10^{14}$ m^{-3}. (*e*) Temperature of the exsolved vapor phase, T_g. (*f*) Dimensionless concentration and temperature profiles across the melt shell at $p_m = 20$ MPa.

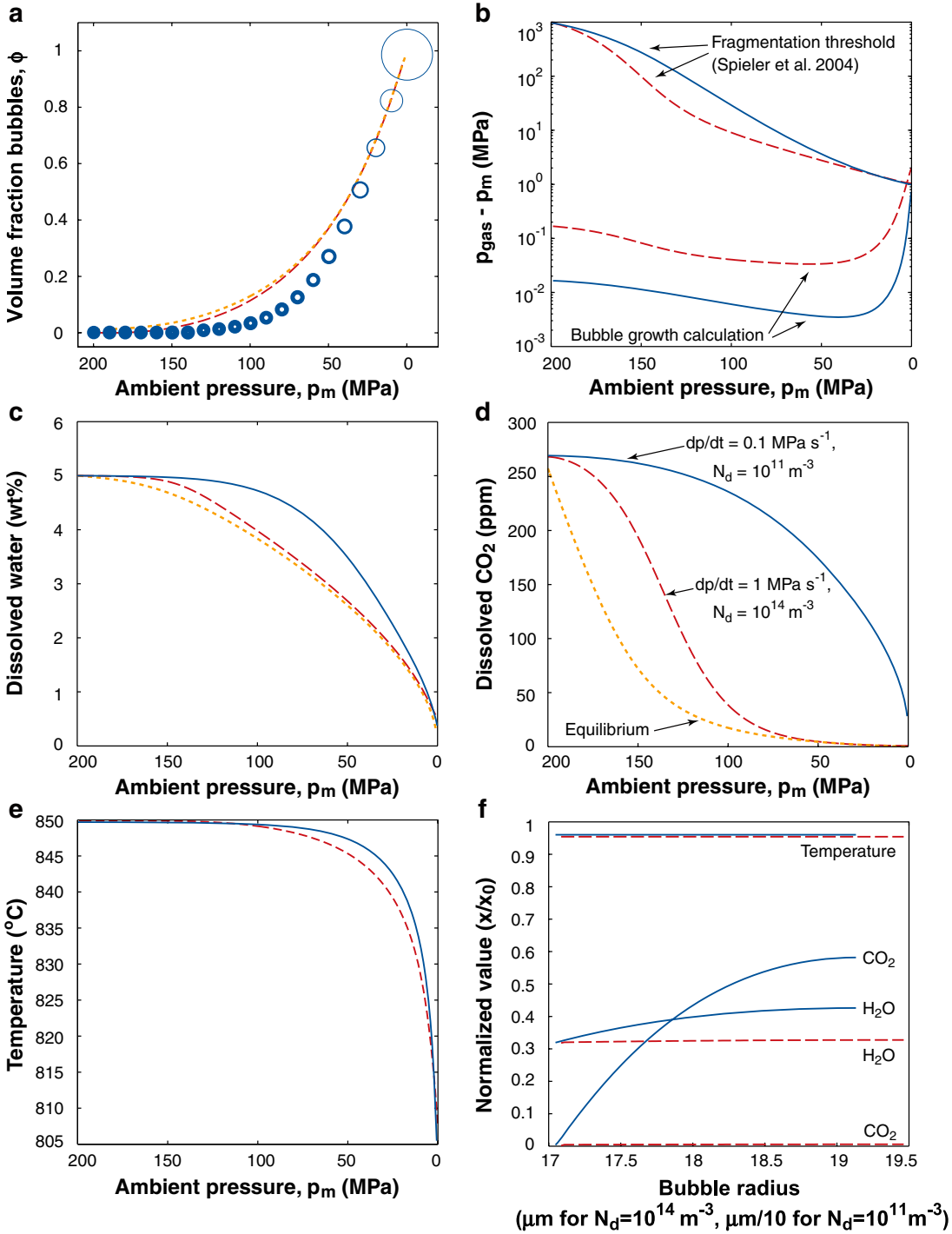

3.2.2. Diffusive limit. During diffusion-limited bubble growth, $\mathrm{Pe}_{dif} = \tau_{dif}/\tau_{dec} \gg 1$ and $p_g - p_m$ is small, where $\tau_{dif} = (S-R)^2/D$, and D is volatile diffusivity. In this limit volatile diffusion through the melt shell is slower than the decompression-driven solubility decrease at the melt-vapor interface. Consequently, the melt becomes supersaturated in volatiles. However, contrary to the viscous limit, supersaturation is not associated with increased p_g. Bubble growth follows a parabolic growth law (Lensky et al. 2004)

$$\hat{R} = \sqrt{\frac{3}{7}\hat{\rho}_m \frac{\tau_{dec}}{\tau_{dif}} c_0 [3(1-\hat{t})^{-2/3} - 7 + 4\sqrt{1-\hat{t}}] + (1-\hat{t})^{-2/3}}, \tag{3}$$

where $\hat{\rho}_m = \rho_m/\rho_{g,0}$ is nondimensional melt density, ρ_m is the melt density, and $\rho_{g,0}$ is the initial gas density. Because of the strong dependence of growth rate on concentration and, hence, supersaturation, late bubble nucleation (i.e., large supersaturation) has the potential for large growth rates.

3.2.3. Solubility limit. During solubility-limited bubble growth the system is close to mechanical and chemical equilibrium (Lensky et al. 1994). In this case $\mathrm{Pe}_{dif} \ll 1$, $\mathrm{Pe}_{vis} \ll 1$ and both overpressure and supersaturation remain small. Equilibrium bubble growth scales with the growth law (Lensky et al. 2004)

$$\hat{R} = \frac{S_{\hat{R}=0}}{R_0}\left(\hat{\rho}_m \frac{c_{\hat{R}=0} - c_0\sqrt{1-\hat{t}}}{1-\hat{t}}\right)^{1/3}. \tag{4}$$

3.2.4. Numerical modeling of bubble growth. Bubble growth experiments (Liu & Zhang 2000, Mader et al. 1994, Mourtada-Bonnefoi & Mader 2001, Navon et al. 1998) demonstrate that real bubble growth includes different stages for which Navon et al. (1998) have provided analytical formulations. However, analytical models cannot account for more realistic (multicomponent) volatile solubility, nor can they capture the dynamic interaction between changes in temperature caused by bubble growth and volatile exsolution, the spatially and temporally varying viscosity of the melt phase, as well as more realistic decompression scenarios. Numerical models of bubble growth permit both the simulation of these realistic complexities and results that can be combined with other processes that occur within the conduit.

Because of the large melt viscosities and short length scales involved, the Reynolds number for bubble growth is $\ll 1$. Therefore, the equation of motion for the spherically symmetric bubble surface, obtained by neglecting inertial terms of the Navier-Stokes equation, is (Lensky et al. 2001)

$$p_g - p_m = 2\frac{\gamma}{R} + 12 v_R R^2 \int_R^S \frac{\eta_{melt}(r)}{r^4} dr. \tag{5}$$

Here v_R is the radial velocity of the melt-vapor interface and γ_{melt} is the Newtonian viscosity of the melt. Mass conservation of volatiles requires that

$$\frac{d}{dt}\left(\rho_g R^3\right) = 3R^2 \rho_m \sum_i D_i \left(\frac{\partial c_i}{\partial r}\right)_{r=R}, \tag{6}$$

where ρ_g is gas density, ρ_m is melt density, D_i is diffusivity of volatile species i in the

melt, and c_i is the mass fraction of the dissolved volatile of species i. Volatile diffusion is governed by (Proussevitch et al. 1993a)

$$\frac{\partial c_i}{\partial t} + v_r \frac{\partial c_i}{\partial r} = \frac{1}{r^2}\frac{\partial}{\partial r}\left(D_i r^2 \frac{\partial c_i}{\partial r}\right), \tag{7}$$

where v_r is the radial velocity of melt at radial position r. Boundary conditions for the diffusion problem are

$$\left(\frac{\partial c_i}{\partial r}\right)_{r=S} = 0 \quad \text{and} \quad c_i(r = R) = f(p_g, T_g, x_i) \tag{8}$$

Here c_i is determined from a solubility model (Liu et al. 2005) and x_i is the mole fraction of volatile species i in the gas phase. Gas expansion and volatile exsolution (latent heat of vaporization) cool the ascending magma, whereas viscous dissipation during bubble growth generates heat. The heat balance for a growing bubble is given by (Proussevitch & Sahagian 1998)

$$\frac{dT_g}{dt} = \Pi\left[\rho_m c_{pm} D_T \left(\frac{\partial T_m}{\partial r}\right)_{r=R} - \sum_i \Delta H_{vi} D_i \rho_m \left(\frac{\partial c_i}{\partial r}\right)_{r=R} + \frac{R}{3}\frac{dp_g}{dt}\right]. \tag{9}$$

Here $\Pi = 4\pi R^2/(n\, c_{pg} M_g)$, c_{pg} is the specific heat of the gas mixture, M_g is the mass of exsolved gas in the bubble, c_{pm} is the specific heat of the melt, D_T is the thermal diffusivity of the melt, T_m is the temperature of the melt, and ΔH_{vi} is the latent heat of vaporization. The first term on the right represents diffusive heat flux from the melt to the gas phase, the second term is the heat of exsolution for volatile species i, and the third term is the change in heat due to expansion of the vapor phase. Diffusion of heat in the melt, with viscous heat generation, is given by (Bird et al. 1960)

$$\frac{\partial T_m}{\partial t} + v_r \frac{\partial T_m}{\partial r} = \frac{1}{r^2}\frac{\partial}{\partial r}\left(D_T\, r^2 \frac{\partial T_m}{\partial r}\right) + \frac{2\eta}{\rho_m c_{pm}}\left[\left(\frac{\partial v_r}{\partial r}\right)^2 + 2\left(\frac{v_r}{r}\right)^2 - \frac{1}{3}\left(\frac{1}{r^2}\frac{\partial}{\partial r}(r^2 v_r)\right)^2\right]. \tag{10}$$

These equations do not account for latent heat of crystallization of the melt or for melt compressibility. Dominant terms in the heat balance are cooling of the melt by decompression of the vapor phase 0(10–100)K for typical rhyolitic magmas (Mastin & Ghiorso 2001, Proussevitch & Sahagian 1998) and diffusion of heat from the melt (0(10–100)K). The effect of gas exsolution is relatively small (0(10)K), whereas viscous heating by bubble growth is negligible. Viscous heating by magma flow in the volcanic conduit is an additional source term and is discussed in Section 4.

Model results show that during instantaneous decompression bubble growth begins with a period of accelerating growth, followed by a period of steady growth and finally a period of decelerating growth (Kaminski & Jaupart 1997, Proussevitch et al. 1993a, Toramaru 1995). Upon instantaneous decompression, bubble growth rates may vary by up to four orders of magnitude, depending on magmatic conditions (Proussevitch & Sahagian 1998). At constant decompression rates, considerable overpressure and oversaturation can be achieved for rhyolitic magmas at sufficiently fast ascent rates (>0.1 MPa/s). Two illustrative model calculations are shown in **Figure 2**, where in addition to H_2O, we also include the (realistic) presence of CO_2 as a second volatile species. Note that there can be considerable diffusive fractionation of CO_2

relative to H_2O as a consequence of the lower diffusivity of CO_2 (Gonnermann & Manga 2005b). Because bubble number density, N_d, determines the thickness of the surrounding melt, nonequilibrium is strongly dependent on N_d (**Figure 2*b*,*c*,*f***). Gas pressure inside bubbles may exceed ambient pressure by up to several megaPascals (**Figure 2*b***). This can be attributed to viscous retardation of bubble growth as magma viscosity increases by volatile exsolution and adiabatic cooling (**Figure 2*e***). We see in Section 3.3 that these high gas pressures may cause explosive eruptions.

Degassing: the loss of dissolved volatile species from the melt phase

3.2.5. Coalescence. The merging of smaller bubbles to make larger ones promotes the separation of gas from the melt because the rise speed of bubbles relative to melt is proportional to R^2. Coalescence depends on melt viscosity and is probably only important in low-viscosity magmas, or more viscous bubbly magmas that are stored in the subsurface for long periods of time.

Coalescence requires the drainage of the melt in the films between two bubbles or the plateau borders between three or more bubbles. Film drainage is dominated by capillary stresses, which scale with γ/R for $R < 1$ cm (Proussevitch et al. 1993b); buoyancy stresses, which scale as $\rho g R$, only dominate for $R > 10$ cm, a size achieved by very few bubbles in magmas. A drainage velocity can be estimated by balancing the pressure gradient γ/R^2 by viscous resistance within the film $\eta_{melt} v/R^2$, where v is the velocity in the film; the length scale in the viscous stress term is the radius R rather than film thickness because the bubble-melt surface is assumed to be a free-slip surface. Thus, $v \sim \gamma/\eta_{melt}$ and highlights the importance of melt viscosity on coalescence. Film drainage is enhanced by shear, either by flow or by expansion of bubbles during decompression (Larsen et al. 2004). The effect of crystals on coalescence is not well characterized, but, as discussed in Section 3.1, if crystals lower surface energy, we should expect crystals to slow coalescence, both because of the lower surface energy and the obstruction of film drainage. Crystals also increase the melt viscosity, which slows film drainage and should slow the rate of coalescence (Klug & Cashman 1994). Once two bubbles coalesce, surface tension causes the ruptured bubble wall to retract. The timescale for returning to a new spherical shape scales with the relaxation time $\eta_{melt} R/\gamma$. For a basalt with $\eta_{melt} \sim 10^2$ Pa s and $\gamma \sim 0.1$ N/m, this time is $O(1)$ s for millimeter-size bubbles.

Volcanic rocks typically contain a power-law or exponential distribution of bubble sizes (Blower et al. 2001). The hallmark of volumetrically significant coalescence is a deviation in the size distribution from a single power-law or exponential distribution to a distribution with a larger-than-expected number of large bubbles (Cashman & Mangan 1994). Such evidence for coalescence is common in low-viscosity basaltic lavas (Herd & Pinkerton 1997). Occasionally coalescence is also found in more viscous magmas, where it is thought to indicate repose periods during magma ascent that provided sufficient time for coalescence (Cashman & Mangan 1994).

3.3. Death: Degassing

Degassing refers to the solubility- and diffusivity-controlled exsolution of volatiles from the melt phase during ascent-driven decompression. If we define individual parcels of ascending magma as a system, then degassing may occur in a closed system.

In this case there is no loss or gain of volatiles by a given magma parcel. In contrast, during open-system degassing (*a*) gas bubbles may migrate from deeper to shallower parts of the magma, (*b*) gas may flow from bubble to bubble through small apertures in the surrounding melt shells, and (*c*) bubble walls may be ruptured during magma fragmentation, allowing gas to escape.

Outgassing: the loss of gas from the magma

Silicic: magma relatively rich in silica

While the detailed degassing history of an individual magma parcel may be complex, gas will ultimately be lost from the magma. This is referred to as outgassing, or open-system degassing. The style of magma outgassing modulates, and may even determine, the eruptive behavior (Eichelberger 1995, Villemant & Boudon 1998, Woods & Koyaguchi 1994). Outgassing probably starts at depth during magma ascent (Jaupart 1998, Taylor et al. 1983). The erupting magma may be outgassed to variable degrees by the time it reaches the earth's surface, where in some cases outgassing may continue until most exsolved gas is lost from the magma (Eichelberger et al. 1986, Westrich & Eichelberger 1994). If outgassing is inefficient on the timescale of the eruption, the bubbly magma may fragment catastrophically into a gas-pyroclast dispersion (Wilson et al. 1980). In this process the potential and thermal energy of the melt and gas phases are converted to kinetic energy (Koyaguchi & Mitani 2005, McBirney & Murase 1970, Namiki & Manga 2005).

3.3.1. Outgassing. In low-viscosity mafic magmas, buoyant bubble rise may result in differential movement of bubbles and melt. Gas bubbles may rise from deeper parts of the magma to accumulate in near-surface storage reservoirs and pathways (Gerlach & Graeber 1985, Hurwitz et al. 2003). Here gas bubbles may eventually rise buoyantly or advect by convective overturn to the surface where they may burst and release gas to the atmosphere. If the magma rise velocity is small relative to the bubble rise speed, bubbles may accumulate and coalesce to produce large gas slugs that fill almost the entire width of the volcanic conduit (Jaupart & Vergniolle 1988, Parfitt 2004). Bursting of these gas slugs characterizes Strombolian eruptions with observed gas:melt volume ratios of the order of 10^5:1 (Blackburn et al. 1976, Wilson 1980). At faster magma ascent rates the difference in rise velocity between bubbles and magma becomes negligible. As a consequence of ascent-driven bubble growth the magma may fragment with observed gas:melt volume ratios close to 10^2:1, and the resultant flow forms lava fountains comprised of a central jet of gas with suspended melt droplets (Parfitt 2004, Parfitt & Wilson 1999).

In contrast, silicic magmas may outgas due to gas flowing through the porous and permeable magma without the requirement of differential movement of bubbles and melt (Edmonds et al. 2003, Eichelberger et al. 1986, Mueller et al. 2005). Some outgassing may also be the consequence of brittle deformation of the ascending magma (Section 3.4.7) allowing gas to escape through fractures within the magma body (Gonnermann & Manga 2003, Rust et al. 2004, Tuffen et al. 2003). If the conduit walls are permeable and at a lower ambient pressure than p_g, gas may escape from the ascending magma laterally to the wall rock (Eichelberger 1995, Jaupart & Allègre 1991). However, because of mineral precipitation by the wall-rock hydrothermal system, it remains controversial to what extent degassing into wall rocks occurs in nature (Boudon et al. 1998). On the other hand, gas flow measurements at active

silicic volcanoes (Wallace et al. 2003) demonstrate that considerable vertical gas flow through the ascending magma does take place (Edmonds et al. 2003).

Individual bubbles in magma are connected through small apertures. Here the melt film separating two bubbles has retracted during incipient bubble coalescence (Klug & Cashman 1996). The topology of the void network in magma and volcanic rocks is different from typical porous media because the aperture that connects individual bubbles governs permeability (Saar & Manga 1999). Porosity-permeability relationships for volcanic rocks (and by inference magmas) are generally based on the Kozeny-Carman equation (Carman 1956) and percolation theory (Mueller et al. 2005, Rust & Cashman 2004, Saar & Manga 1999). Generally, they are of the form

$$k(\phi) = \chi(\phi - \phi_{cr})^{\beta}, \tag{11}$$

where χ is an empirical constant, $\phi = (R/s)^3$ is the bubble volume fraction, ϕ_{cr} is the critical bubble volume fraction (percolation threshold), and typically $2 \leq \beta \leq 4$. Permeability measurements indicate that microfractures can play an important role in gas flow through cold lava samples (Mueller et al. 2005). Thus, an uncontroversial permeability model for vesicular magma remains elusive (Takeuchi et al. 2005). Moreover, it is likely that upscaling from lab samples to conduits will need to account for gas flow through fractures (Edmonds et al. 2003). Our compilation of permeability measurements in silicic volcanic rock and magma samples shown in **Figure 3** illustrates a very large range in permeability, implying that complex outgassing behavior should be expected in nature.

3.3.2. Fragmentation. Magma fragmentation is thought to occur over a relatively narrow depth interval at the fragmentation surface (**Figure 1**). Traditionally, it had been assumed that fragmentation occurs at a critical volume fraction, presumably due to the instability of thin bubble walls (Gardner et al. 1996, Verhoogen 1951). Koyaguchi & Mitani (2005) suggest that such "expansion fragmentation" may only be applicable to low-viscosity magmas, consistent with analog experiments (Ichihara et al. 2002, Mader et al. 1994, Martel et al. 2000). There is, however, no clear physical evidence for the general applicability for this criterion, as vesicularity of magma fragments can range from 0 (obsidian) to >98% (reticulite). Namiki & Manga (2005) demonstrate how an expansion fragmentation criterion may derive from the potential energy of the bubbly fluid. Potential energy, a function of ϕ and $\Delta p = (p_g - p_m)$, determines the expansion velocity of the bubbly fluid. Based on the assumption that bubble walls break when strain, also a function of ϕ and Δp, exceeds a critical value, they determine a criterion for the rupture of the elastic bubble walls in terms of ϕ and Δp. This criterion is similar to the "stress criterion," based on the view that fragmentation in high-viscosity magmas occurs when magma overpressure is sufficiently large to rupture bubble walls (Alidibirov 1994, McBirney & Murase 1970, Zhang 1999). The stress criterion is a functional relation between the tensile strength of the melt, σ_{melt}, the critical overpressure for fragmentation, Δp_{fr}, and ϕ. A recent formulation with good fit to a broad range of experimental data for real magmas is provided by Spieler et al. (2004)

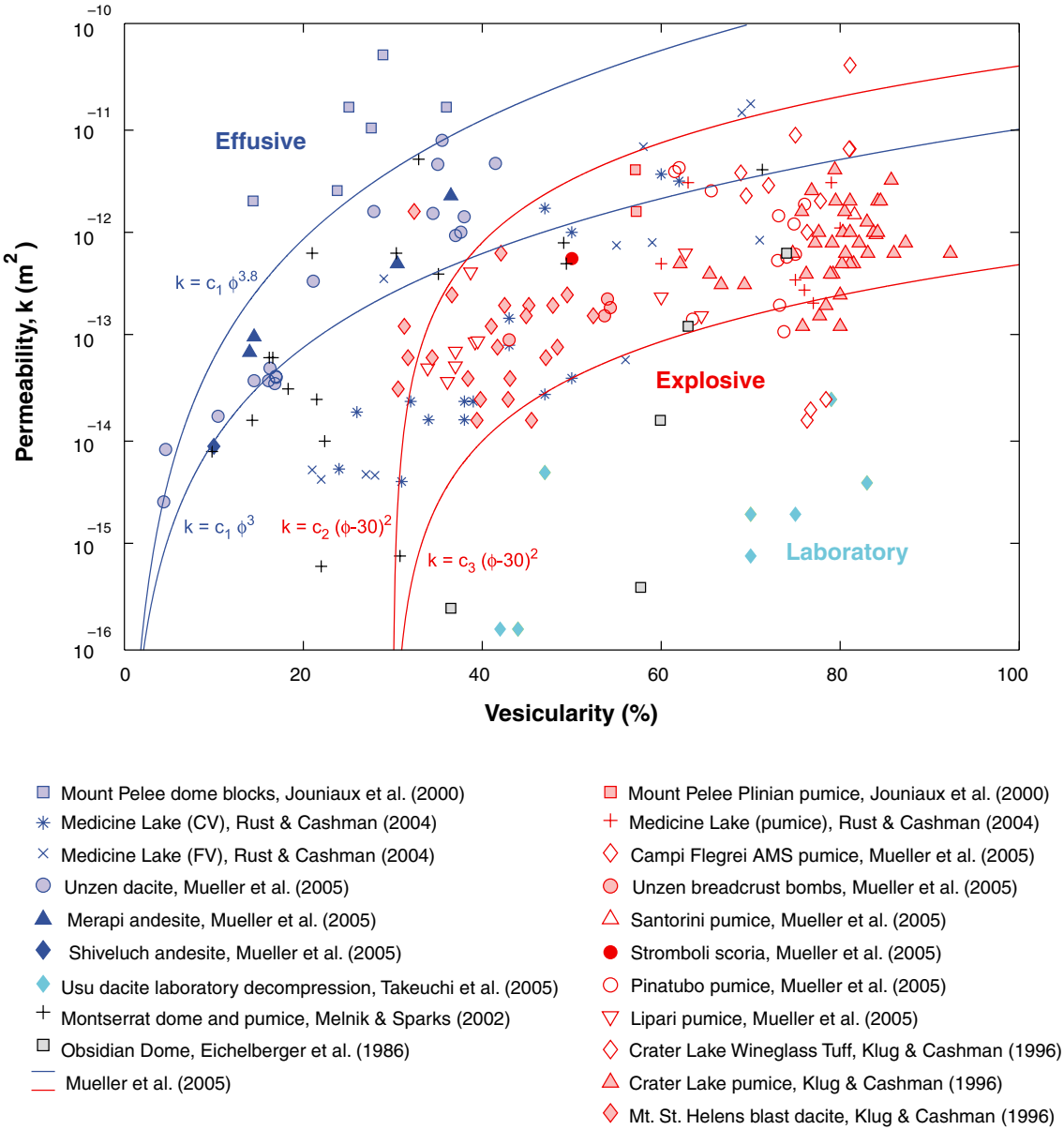

Figure 3

Porosity-permeability measurements of silicic volcanic rocks and melt. Measurements are published in Eichelberger et al. (1986), Jouniaux et al. (2000), Klug & Cashman (1996), Melnik & Sparks (2002), Mueller et al. (2005), Rust & Cashman (2004), and Takeuchi et al. (2005).

$$\Delta p_{fr} = \sigma_{melt}/\phi. \tag{12}$$

Figure 2*b* shows Δp, as well as the required overpressure Δp_{fr} for fragmentation based on Equation 12. The buildup of sufficient overpressure for fragmentation occurs in the viscous limit. Hence, it depends primarily on decompression rate and typically occurs in the upper part of the conduit.

An alternative to the stress criterion is the strain-rate criterion (Dingwell 1996, Papale 1999b), which postulates that strain rates at the fragmentation surface exceed the structural relaxation rate of the magma or melt phase

$$\dot{\epsilon}_g > K\frac{1}{\tau_s} = K\frac{G}{\eta_{melt}}, \tag{13}$$

where $K = O(10^{-2})$, τ_s is the structural relaxation time discussed in Section 3.4.3, and the melt viscosity is measured at low strain rates.

3.4. Magma Rheology

The rheology of magmas is extremely variable, with viscosities ranging over many orders of magnitude, often within a single volcanic eruption. Factors that affect the rheological behavior include (*a*) the chemical composition of the melt phase, (*b*) the volatile-dependent viscosity of the melt phase, (*c*) the magma temperature, (*d*) the volume fraction and size of gas bubbles, (*e*) the volume fraction and shape of crystals, and (*f*) the rate of magma deformation.

3.4.1. Chemical composition and molecular structure of silicate melts. The structure of silicate (SiO_2-dominated) melts and glasses is a disordered, three-dimensional network of interconnected SiO_4 tetrahedra. The rearrangement of the average molecular structure of a silicate melt is known as structural relaxation and involves breaking and remaking of Si-O bonds, in other words a self-diffusive motion of atoms. While the local structure is continually rearranging, the average structure of a melt is constant with time, akin to a dynamic equilibrium. This continual structural rearrangement is in part responsible for the viscous character of silicate melts (Moynihan 1995). The degree of polymerization determines the intrinsic viscosity of silicate melts, which can vary over orders of magnitude with chemical composition or volatile content (Giordano & Dingwell 2003).

3.4.2. Dissolved volatiles and temperature. In most magmas water is the dominant volatile species. It dissociates into molecular water and hydroxyls when it dissolves and disrupts the bridging oxygens of the silicate network. For rhyolitic melts, Hess & Dingwell (1996) developed a widely used empirical viscosity model. Viscosity varies by several orders of magnitude for typical water contents and temperatures observed in rhyolitic magmas (**Figure 4**). Similar dependencies are observed for other melt compositions (Russell et al. 2002), but with a less pronounced dependence on volatile content for more mafic magmas.

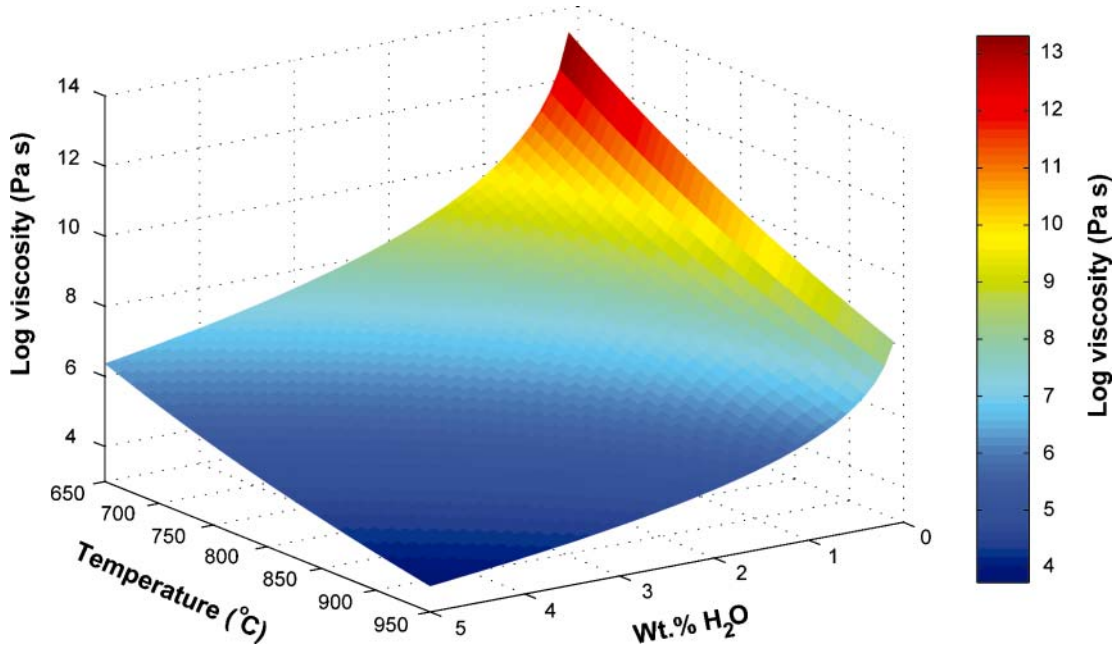

Figure 4

Dependence of silicate melt (leucogranite) viscosity on temperature and water content, after the empirical formulation of Hess & Dingwell (1996).

3.4.3. Strain-rate dependence. Silicate melts respond to applied forces with viscous deformation. This is a consequence of structural relaxation (Moynihan 1995) and can be characterized by the flow relaxation rate $\dot{\epsilon}_r$ (Moynihan 1995; Webb & Dingwell 1990a,b; Yue & Brückner 1994). At small deformation rates ($\dot{\epsilon} \ll \dot{\epsilon}_r$) the melt is in a fully "relaxed" state, corresponding to Newtonian flow. At $\dot{\epsilon} \sim \dot{\epsilon}_r$ the flow becomes shear-thinning, with a strain-rate-dependent (SRD) viscosity defined as η/η_{rel}, where η_{rel} is the Newtonian (relaxed) melt viscosity and η is the measured viscosity. Finally, at high deformation rates ($\dot{\epsilon} \gg \dot{\epsilon}_r$) the induced relative motions of structural units are no longer compensated by random reordering of bridging oxygens, resulting in structural (brittle) failure of the melt.

SRD viscosities of silicate melts of a wide range of compositions and temperatures appear to have a similar dependence on the dimensionless strain rate, $\dot{\epsilon}^* = \dot{\epsilon}\tau_s$ (**Figure 5**), where $\tau_s = \eta_{rel}/G$ is the structural relaxation time with a shear modulus $G \sim 10^{10}$ Pa (Simmons 1998; Webb & Dingwell 1990a,b; Yue & Brückner 1994). Measured viscosities are well represented by the SRD equation (Simmons 1998)

$$\frac{\eta}{\eta_{rel}} = (1 + \eta_{rel}\dot{\epsilon}/\sigma_\infty)^{-1}. \quad (14)$$

Here $\sigma_\infty \propto \eta_{rel}^{0.24}$ is the maximum shear (cohesive) strength that can be supported by the melt (Simmons 1998). In the SRD equation it is assumed that viscous

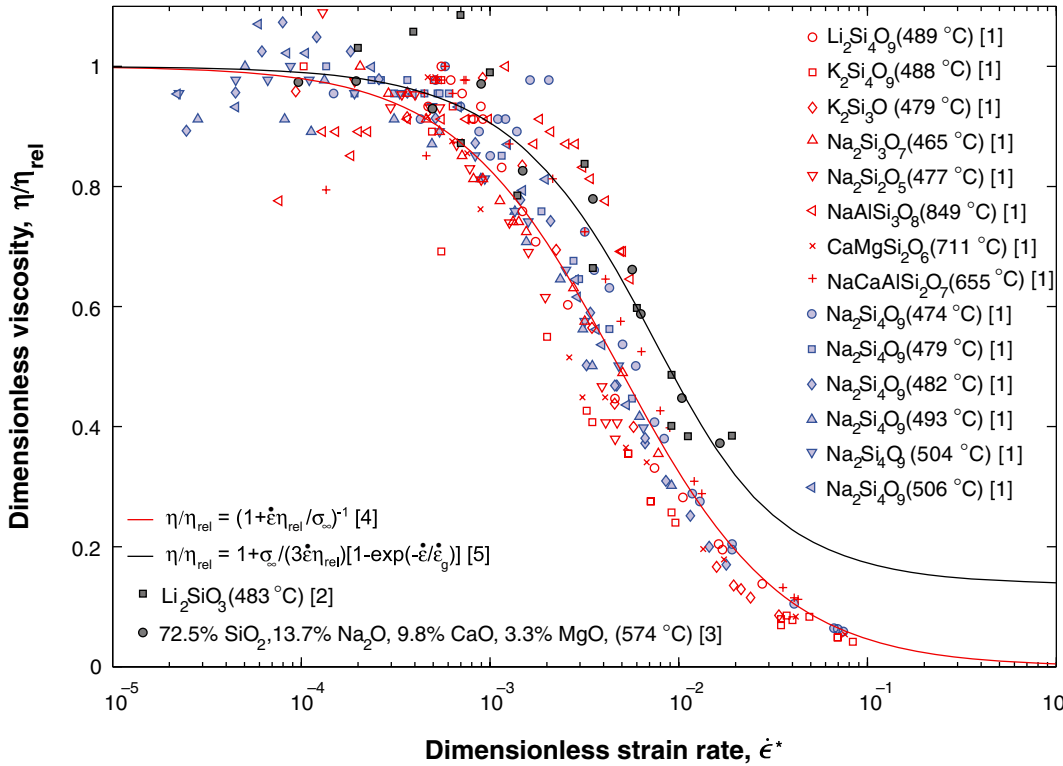

[1] Webb & Dingwell (1990)
[2] Deubener & Brückner (1997)
[3] Thies (2002)
[4] Simmons et al. (1982)
[5] Brückner & Yue (1994)

Figure 5

Strain-rate-dependent viscosity of silicate melts. Measurements are published in Brückner & Yue (1994), Deubener & Brückner (1997), Simmons et al. (1982), Thies (2002), and Webb & Dingwell (1990b).

heating during viscosity measurements is negligible. Yue and Brückner (1994) derive an alternative formulation that includes a correction for viscous heating.

Glass transition: a change in melt behavior from a viscous to a hard, brittle material

3.4.4. Glass transition. The transition from viscous flow to structural failure is called the glass transition. It is characterized by a time-temperature curve that may be crossed from viscous to brittle behavior either by cooling or by decreasing the deformational timescale. It can be defined in terms of the structural relaxation time, where η_{rel} depends on temperature and the glass transition temperature, T_g, which depends on melt composition (Knoche et al. 1994) and strongly decreases with increasing water content (Deubener et al. 2003). Over a wide range of water contents,

T_g, normalized to its value at a low water content is the same for a broad range of melt compositions (Deubener et al. 2003).

For a wide range of silicate melts and temperatures, structural failure occurs at the critical strain rate $\dot{\epsilon}_g \sim 0.01/\tau_s$ (Webb & Dingwell 1990b). If the melt contains gas bubbles, brittle failure occurs at even lower strain rates (Thies 2002). Because of the potential for a transition from viscous flow to brittle failure during magma ascent, the dependence of the glass transition on the applied strain rate is important in volcanic eruptions (Dingwell 1996, Webb & Dingwell 1990a).

3.4.5. Bubbles. Magma viscosity (melt + bubbles) differs from that of the melt phase alone. At low strain rates surface tension exceeds viscous forces, that is the Capillary number $\mathrm{Ca} = \eta_{melt}\dot{\epsilon}R/\gamma < 1$, and bubbles remain nearly spherical. During magma flow melt has to flow around bubbles, resulting in a net increase in the viscosity of the magma compared with the melt viscosity. At sufficiently high strain rates ($\mathrm{Ca} > 1$), bubbles become elongated and a significant component of magma deformation is accommodated by bubble deformation and slip at the melt-vapor interface, a free-slip surface. Consequently, magma viscosity is decreased relative to the melt viscosity. Empirical viscosity formulations for vesicular silicate melts (Bagdassarov & Dingwell 1992, Stein & Spera, Thies 2002) and other liquid-bubble suspensions at $\mathrm{Ca} \gg 1$ and at $\mathrm{Ca} \ll 1$ (Llewellin & Manga 2005, Rust & Manga 2002) are summarized in **Figure 6**.

3.4.6. Crystals. Owing to decompression and cooling, crystals nucleate and grow in the ascending magma (Couch et al. 2003, Hammer et al. 1999, Hammer & Rutherford 2002). This not only changes the chemical composition and dissolved volatile content of the melt phase, but also affects the overall rheology of the magma. At crystal fractions of less than approximately 40 vol %, the effect of crystals on viscosity is similar to that of bubbles at $\mathrm{Ca} \ll 1$ (**Figure 6**), and reduced viscosities for both suspensions are well represented by a relation of the type $(1-\phi/\phi_*)^\alpha$, albeit with different exponents. Here ϕ_* represents a critical volume fraction at which crystals start to impede flow of the suspension. At a crystal content greater than approximately 40 vol %, a rheological transition occurs to a regime where the effect of crystals dominates and the suspension behaves like a Bingham fluid with a yield strength (Lejeune & Richet 1995). This is thought to be the consequence of the formation of a continuous crystal network and is expected to depend on the aspect ratio of nonspherical crystals (Saar et al. 2001). In experiments with silicate melts at high crystal fractions deformation becomes inhomogeneous with the formation of shear zones and catastrophic failure (Lejeune & Richet 1995). Some rheological formulations that extend into this regime exist (Costa 2005), but probably require further experimental calibration. As illustrated in **Figure 7**, the SRD rheology of melt with suspended bubbles and crystals derives from a superposition of the individual dependencies (Brückner & Deubener 1997, Thies 2002).

3.4.7. Brittle failure. Under shear or elongation at sufficiently high strain rates silicate melts no longer deform viscously, but instead deform in a brittle manner. For

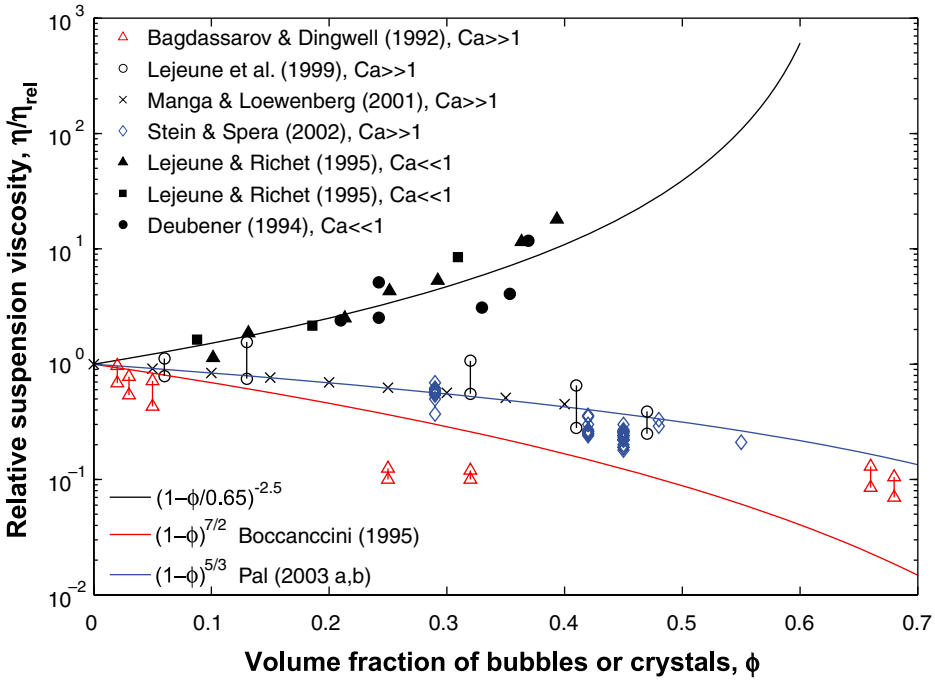

Figure 6

Relative viscosity of suspensions of silicate melt + bubbles (*open triangles*, *circles*, and *diamonds*) and silicate melt + crystals (*black solid dots*, *triangles*, and *squares*). Only cases with Ca $\ll 1$ and Ca $\gg 1$ are shown. Crosses are numerical calculations for bubbles in liquid (Manga & Loewenberg 2001). Note that at values of ϕ above approximately 0.4 the rheological behavior for melt and crystals becomes complex and inhomogeneous, including yield strength and shear localization (see Lejeune & Richet 1995 for a discussion). Measurements are published in Bagdassarov & Dingwell (1992), Deubener (1994), Lejeune et al. (1999), Lejeune & Richet (1995), Manga & Loewenberg (2001), and Stein & Spera (2002).

pure melts, this change in rheological behavior occurs at the glass transition. In the presence of vesicles the critical strain rate deceases with increasing vesicularity (Thies 2002), whereas the presence of crystals, at least at low volume fractions, appears to be negligible (Thies 2002).

4. CONDUIT FLOW

Dynamical models of volcanic eruptions demonstrate that feedback between various processes within the conduit and the magma chamber can lead to nonlinear eruptive behavior (Melnik & Sparks 1999). Ultimately, it appears that the eruptive style—explosive or effusive—is largely controlled by the magma flow rate (Cashman & McConnell 2005, Scandone & Malone 1985, Woods & Koyaguchi 1994), which is modulated by processes within the volcanic conduit. Here we illustrate the relative importance of the dominant conduit processes in a simplified model of silicic magma

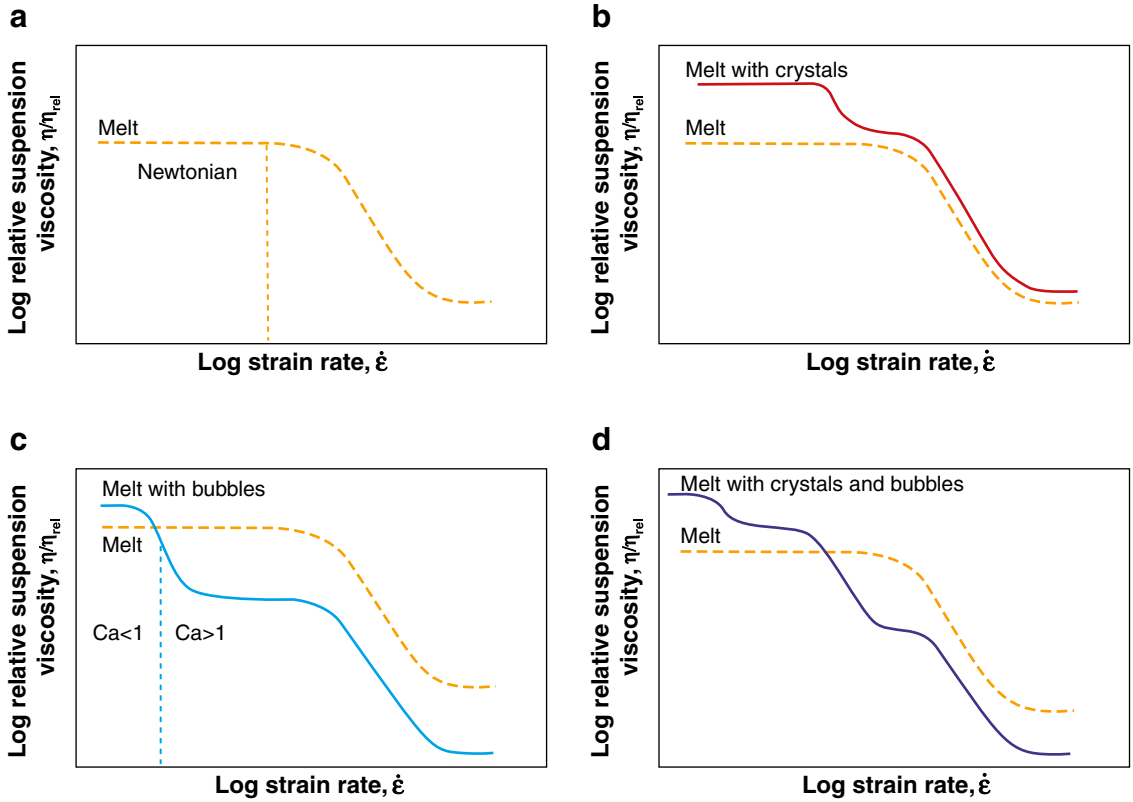

Figure 7

Schematic relative suspension viscosity as a function of strain rate for (*a*) pure melt, (*b*) melt with crystals, (*c*) melt with bubbles, and (*d*) melt with bubbles and crystals. Modified from Thies (2002).

ascent below the fragmentation surface. The processes we consider are: (*a*) volatile supersaturation and secondary bubble nucleation during diffusive bubble growth, (*b*) shear brecciation of magma near the conduit walls, (*c*) shear heating leading to shear localization, (*d*) permeable gas flow during volatile exsolution, and (*e*) buildup of overpressure inside bubbles that leads to magma fragmentation.

In our calculations we assume a constant mass flux through a vertical cylindrical conduit of uniform radius a. Constant conduit diameter is a simplification employed in most conduit models. It may be a good approximation close to the surface, but at greater depths magma may rise in planar dikes (Carrigan 2000, Jaupart 2000). Assuming a constant mass flux eliminates the dynamical feedback between the magma chamber and conduit flow. This permits a direct examination of the various mechanical processes associated with magma flow in the conduit. Constant mass flux is a good approximation for long-lived effusive silicic eruptions and sub-Plinian or

Plinian eruptions with eruption durations that are longer than magma ascent times from chamber to surface.

4.1. The Conduit Model

We account for radial and vertical variations in bubble growth, temperature, and magma rheology. For mass flux less than 10^8 kg s^{-1}, flow below the fragmentation surface is expected to be laminar (Reynolds number, $Re < 10^2$). The vertical component of velocity (u_z) varies more slowly in the vertical than the radial direction (Mastin 2005). The vertical component of velocity (u_z) varies more slowly in the vertical (z) than in the radial direction (r) of the conduit. We therefore neglect $\partial u_z/\partial z$ and treat the magma flow problem as laminar, as well as incompressible and steady (Mastin 2005)

$$\sigma_{zr} = -\frac{r}{2}\left(\frac{\partial p_m}{\partial z} + \rho g\right) = -\eta\frac{du_z}{dr}, \tag{15}$$

with

$$u_r = u_\theta = 0, \tag{16}$$

$$\sigma_{rr} = \sigma_{\theta\theta} = \sigma_{zz} = \sigma_{r\theta} = \sigma_{z\theta} = 0, \tag{17}$$

$$\left(\frac{du_z}{dr}\right)_{r=0} = (u_z)_{r=a} = 0, \tag{18}$$

$$\frac{\partial\rho}{\partial r} = \frac{\partial\rho}{\partial\theta} = \frac{\partial p_m}{\partial r} = \frac{\partial p_m}{\partial\theta} = 0, \tag{19}$$

$$\rho = (1-\phi)\rho_m + \phi\rho_g, \tag{20}$$

$$\int_A u_z \rho dA = \dot{Q}_m. \tag{21}$$

Here σ_{ij} are the components of the stress tensor in cylindrical coordinates, a is the conduit radius, θ is the circumferential direction, n is the strain-rate-dependent magma (melt + bubbles) viscosity, ρ_g is the density of the gas phase, ρ_m is the melt density, and A is the conduit cross-sectional area. Magma density decreases as bubbles grow, and the average magma velocity increases simultaneously. Bubble growth is based on the formulation of Section 3.2. Magma viscosity depends on volatile content, temperature, and shear strain rate, as described in Sections 3.4.2, 3.4.3, and 3.4.5. Shear heating of magma is calculated using the simplified energy equation

$$\frac{DT_m}{Dt} = \left[D_T\left(\frac{\partial^2 T_m}{\partial r^2} + \frac{1}{r}\frac{\partial T_m}{\partial r}\right) - \frac{1}{\rho_m c_{pm}}\left(\sigma_{rz}\frac{\partial u_z}{\partial r}\right)\right]. \tag{22}$$

The last term in Equation 22 represents shear heating (viscous dissipation). By lowering viscosity, it will change the velocity distribution across the conduit and will reduce the resistance to flow. The relative importance of shear heating and heat conduction

can be characterized by a Brinkman number

$$\mathrm{Br} = \frac{\eta \dot{Q}_m^2}{c_{pm} \rho_m^3 D_T \Delta T a^4 (1-\phi)^2} \tag{23}$$

where ΔT is the temperature increase at which viscosity changes by an appreciable amount. Because of the nonlinearity of η and u_z determining a critical value of Br is not straightforward and we focus on dimensional values in the following. Initial conditions, denoted by a subscript 0, are $T = 850^\circ$C, $\phi_0 = 1\%$, $c_{w,0} = 5$ wt.%, $a = 25$ m, $c_{c,0} = 268$ ppm, $x_c = 0.21$, $p_{m,0} = 200$ MPa. We vary bubble number density between $10^9\,\mathrm{m}^{-3} \leq N_d \leq 10^{15}\,\mathrm{m}^{-3}$ and mass flux between $10^5\,\mathrm{kg\,s}^{-1} \leq \dot{Q}_m \leq 10^8\,\mathrm{kg\,s}^{-1}$.

Wherever the shear strain rate exceeds that required for brittle deformation (Section 3.4.7), we predict the occurrence of brittle shear deformation. Because no further insight can be gained within the present framework, we refrain from modeling this process, for example with an ad hoc viscosity reduction. The ambient pressure at which fragmentation is first predicted to occur is based on the criterion of Spieler et al. (2004). Because of the significantly lower wall friction associated with the high-Re flow of the gas-pyroclast mixture above the fragmentation surface, pressures of the order of 10 MPa at the fragmentation surface correspond to depths of several kilometers (Koyaguchi 2005, Woods 1995), (**Figure 8*b***).

We predict outgassing through the permeable magma as a dominant process when the rate of upward gas flux exceeds the calculated rate of gas exsolution (Section 3.2)

$$\dot{Q}_g \leq \frac{\rho_g k}{\eta_g} \left(\frac{dp_g}{dz} \right). \tag{24}$$

Here permeability, $k = \chi \phi^{2.7}$ with $\chi = 10^{-11}\,\mathrm{m}^2$ (Section 3.3) and η_g is the gas viscosity.

In order to solve the equations that describe flow in the conduit we solve two coupled problems. At a subgrid scale we model diffusive bubble growth following the method outlined in Proussevitch et al. (1993) and Proussevitch & Sahagian (1998), where the diffusion of volatiles through the expanding melt shell is calculated in a Lagrangian reference frame (Equations 5–10). This subgrid model determines ϕ and η_{rel} required for the solution of the magma flow problem. Magma flow is obtained by solving Equations 15–22 in the radial direction using finite differences and an explicit advection scheme for the vertical direction. Bubble growth and magma flow are also coupled via the pressure boundary condition (p_m of Equation 5). Consequently, bubble ascent (decompression) is also solved in a Lagrangian reference frame based on the advection scheme for the flow problem. The fragmentation depth is obtained from Equation 29 in Koyaguchi (2005). Similar to Mastin (2005) we neglect $u_z \frac{\partial T}{\partial z}$ in Equation 22.

A simulation of the evolution of model parameters with ascent is shown in **Figure 9**. For this specific case, fragmentation occurs when the pressure difference $p_g - p_m$ reaches the fragmentation threshold (**Figure 9*c***). At this point viscosity has increased by three orders of magnitude owing to degassing, and vesicularity has reached about 0.9.

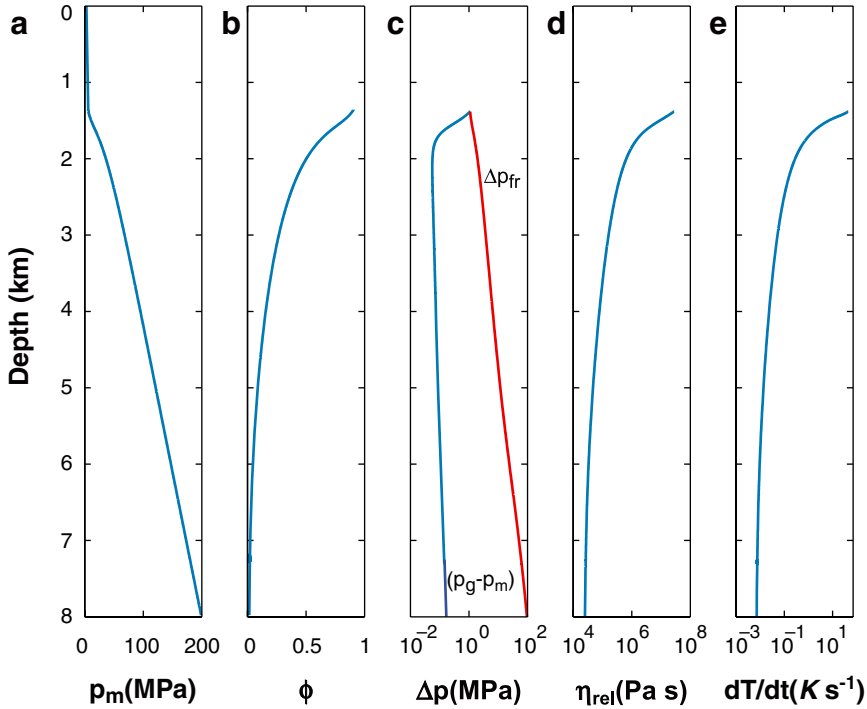

Figure 8

Model variables as a function of depth for $\dot{Q}_{mass} = 10^{7.5}$ kg s^{-1}, $a = 25$ m, and $N_d = 10^{15}$ m^{-3}. (*a*) p_m is the sum of magma-static (weight of magma) and dynamic pressure loss. Above the fragmentation depth pressure loss is assumed to be linear. (*b*) ϕ is shown at the conduit center. (*c*) $p_g - p_m$ (*blue*) and fragmentation overpressure Δp_{fr} (Spieler et al. 2004) (*red*). When $\Delta p_{fr} = (p_g - p_m)$ fragmentation is predicted to occur. (*d*) Relaxed, Newtonian melt viscosity, η_{rel}. (*e*) Viscous heating at the conduit wall becomes significant a few hundred meters below the fragmentation depth.

4.2. Conduit Flow Regimes

Figure 9 summarizes the results from model calculations for two end-member cases of N_d and a range of $\dot{Q}_m$. Curves show the point at which a given flow-related process is first predicted to occur or become dynamically significant. **Figure 9*a*** is for an end-member case representative of volcanic eruptions producing pumice of low bubble number density ($N_d \sim 10^9$ m^{-3}), or alternatively for deeper portions of conduit flow prior to secondary bubble nucleation events (Massol & Koyaguchi 2005). **Figure 9*b*** is an end-member scenario representative of eruptions with high initial bubble number densities ($N_d \sim 10^{15}$ m^{-3}), or after secondary bubble nucleation has resulted in high N_d.

4.2.1. Secondary nucleation and explosive fragmentation. Bubble number density, N_d, controls the ability of volatiles to exsolve efficiently. At low N_d and large $\dot{Q}_m$ bubble growth is diffusion limited ($\mathrm{Pe}_{dif} \gg 1$). Supersaturation builds up and

secondary bubble nucleation occurs (Sections 3.1 and 3.2, **Figure 9*a***). The dependence on N_d for the transition to diffusion-limited bubble growth (Gonnermann & Manga 2005b) occurs at

$$\dot{p}_m(p_{m,0}\, N_d^{2/3}\, D)^{-1}\, s \sim 1, \tag{25}$$

where s is the solubility constant. **Figure 9*a*** shows that for small bubble number density and mass flow rates $>\sim 10^6$ kg s $^{-1}$ supersaturation and secondary bubble nucleation are expected to occur before other processes become important. Hence, for low-N_d magma ascending at sufficiently large $\dot{Q}_m$, secondary bubble nucleation drives the flow toward a high-N_d regime, as indicated by the circled "N" on **Figure 9**. At large N_d diffusion of volatiles into growing bubbles allows the melt to remain close to equilibrium ($\mathrm{Pe}_{dif} \ll 1$) and no additional nucleation events occur (**Figure 9*b***). Magma continues to ascend until bubble growth becomes viscosity limited ($\mathrm{Pe}_{vis} \gg 1$), resulting in buildup of bubble overpressure and explosive fragmentation (Equation 12). This is indicated by the circled "F" in **Figure 9*b***.

4.2.2. Outgassing. At low $\dot{Q}_m$ magma ascent is dominated by permeability-controlled outgassing (**Figure 9**). Bubble growth eventually results in sufficient permeability (**Figure 3**) for permeable gas flux to balance or exceed the rate of volatile exsolution. Overpressure cannot build up and no explosive fragmentation can occur. At large $\dot{Q}_m$ permeable gas flux is insufficient to balance decompression-driven volatile exsolution (Woods & Koyaguchi 1994).

4.2.3. Influence of rheology. As volatiles exsolve and viscosity increases, ascending magma near the conduit margins where shear strain rates are largest may be subjected to non-Newtonian, shear-thinning behavior (**Figure 7**). At $\dot{Q}_m \leq 10^7$ kg s $^{-1}$ and ambient pressures of the order of 10 MPa, brittle shear deformation of magma is predicted (**Figure 9**). Locally, this may enhance magma permeability and outgassing (Gonnermann & Manga 2003, Jaupart 1998, Tuffen et al. 2003). When shear stresses are relaxed, brecciated magma can become welded and deform viscously again. Thus, there is the potential for repeated cycles of brittle-to-viscous deformation, and textural evidence in some obsidian suggests multiple episodes of brittle deformation (Gonnermann & Manga 2003, 2005a; Rust et al. 2004; Tuffen et al. 2003). It has been suggested that such brittle shear deformation may also be a trigger mechanism for low-frequency seismicity during volcanic eruptions (Goto 1999, Neuberg et al. 2006, Tuffen et al. 2003).

At $\dot{Q}_m \geq 10^7$ kg s $^{-1}$ viscous shear heating reduces magma viscosity before brittle shear deformation can occur. Because of the strong temperature dependence of magma viscosity (**Figure 4**) and the dependence of viscous heating on $(\partial u_z/\partial r)^2$, there is a positive feedback between shear localization near the conduit walls and viscous heating. This reduces the pressure gradient required for magma ascent (Mastin 2005, Vedeneeva et al. 2005) and may be a key mechanism enabling sustained high-intensity explosive eruptions for magma-chamber overpressures of the order of 10 MPa (Stasiuk et al. 1993, Woods & Koyaguchi 1994). It may also contribute to the unsteady behavior of many explosive volcanic eruptions (Costa & Macedonio 2005).

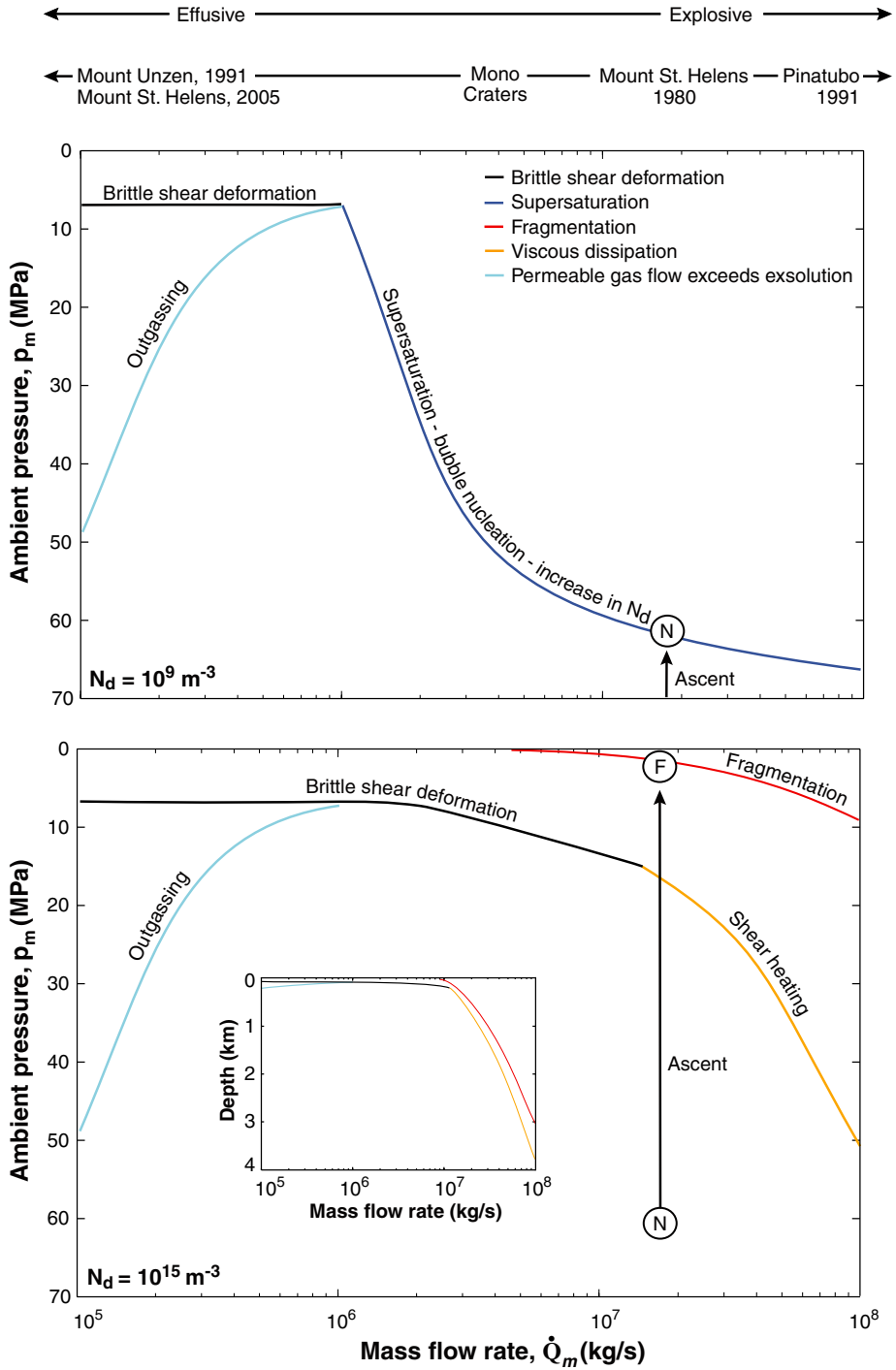

Viscosity reduction by viscous heating moves the magma away from the glass-transition despite increasing shear rates. Hence, brittle shear deformation is unlikely to occur. However, note that pumice textures thought to have formed as a consequence of shear heating and localization may bear evidence for brittle deformation during explosive eruptions with high $\dot{Q}_m$. (Polacci et al. 2005, Rosi et al. 2004).

4.2.4. Eruptions of two distinct magmas. Volcanoes sometimes erupt two or more distinct magma types, either sequentially or simultaneously. Often, one of the two magmas is much more viscous or crystal-rich than the other. The eruption of a precursory, less viscous magma may permit the ascent of the more viscous magma from a magma chamber by reducing the overpressure needed to initiate the eruption (Takeuchi 2004). For simultaneous eruption, the less viscous magma can migrate to the edge of the conduit where it lubricates the more viscous magma and hence decreases the pressure gradient need for ascent (Carrigan & Eichelberger 1990). Less viscous, volatile-rich magma also plays an important role in the replenishment of partially crystallizing magma chambers, where it may result in remobilization of the crystal-rich magma (Zellmer et al. 2003). However, ongoing eruptions at Monserrat (**http://www.mvo.ms**) and Mount St. Helens (**http://vulcan.wr.usgs.gov/Volcanoes/MSH**) are relatively homogeneous, crystal-rich magmas with no obvious role of a much less viscous magma.

4.2.5. Models vs. real volcanoes. Real volcanoes are more complex in several important ways. First, eruptions are unsteady (Mason et al. 2006). They not only have a beginning and an end, but eruption style and the composition of erupted magma (and, hence, physical properties) can change during the eruption, especially during explosive eruptions when the fragmentation surface may fluctuate considerably in depth. To date, there are several competing hypotheses for the fragmentation criterion that determines the fragmentation depth in numerical models (Koyaguchi 2005). Both explosive and effusive eruptions sometimes display periodic variations in discharge and eruption style (Swanson & Holcomb 1990, Voight et al. 1999). In low-viscosity basaltic magmas, periodic explosions can be attributed to the bursting of large gas

Figure 9

Conduit flow regimes for $N_d = 10^9$ m^{-3} (*top*) and $N_d = 10^{15}$ m^{-3} (*bottom*). Vertical axis is ambient pressure, p_m, (depth in inset) and horizontal axis is mass flow rate, $\dot{Q}_m$. Conduit radius is $a = 25$ m. For $\dot{Q}_m < 10^6$ kg s^{-1} degassing is solubility limited. The rate of permeable gas flow through the vesicular magma eventually exceeds the rate of volatile exsolution so that significant outgassing occurs. Eventually, magma viscosity becomes sufficiently large for brittle shear deformation near the conduit walls. At $\dot{Q}_m > 10^6$ kg s^{-1} supersaturation ($\mathrm{Pe}_{dif} \gg 1$) leads to secondary bubble nucleation (*labeled N*) and a shift to larger N_d (*top*). Upon further ascent, viscous heating near the conduit walls results in shear localization and prevents the occurrence of shear brecciation. Finally, overpressure ($\mathrm{Pe}_{vis} \gg 1$) results in fragmentation (*labeled F*) at $p_m \sim 10$ MPa, which is equivalent to several kilometers below the surface, because of the low wall friction of the gaseous flow above the fragmentation depth.

bubbles and slugs, with the interval between eruptions characterizing the time needed to accumulate and form large bubbles (Vergniolle & Jaupart 1990). In more viscous silicic magmas it has been proposed that unsteady flow can be induced because of stick-slip behavior at the conduit walls (Denlinger & Hoblitt 1999). Shear brecciation may be one mechanism to produce stick-slip behavior. Alternative hypotheses include the temperature dependence of magma rheology (Whitehead & Helfrich 1991) and the coupling of magma rheology to crystallization (Mourtada-Bonnefoi et al. 1999) and vesiculation (Wylie et al. 1999). In particular, the feedback between degassing, bubble and crystal nucleation and growth, viscous heating, and magma rheology enables multiple steady-state conduit flow solutions, and, hence, the possibility of periodic eruptions (Costa & Macedonio 2002, Melnik & Sparks 1999). Time-varying processes in the conduit are coupled to the boundary conditions that govern magma ascent, namely the pressure in the magma chamber and elastic deformation of conduit walls, which further modulate cyclic behavior (Barmin et al. 2002) or initiate changes in eruption style (Woods & Koyaguchi 1994).

Second, the conduit itself is a dynamic structure that opens and closes. Conduit shape changes with depth, typically having sheet-like geometry at depth with a cylindrical conduit forming only near the surface (Mitchell 2005, Rubin 1995). The transition in shape causes large variation in ascent rate and hence in processes controlled by the decompression rate and strain rate.

Third, as magma ascends, the loss of volatiles and decrease of pressure promote crystallization (Hammer & Rutherford 2002, Toramaru 1991). The volume fraction of crystals can sometimes exceed 50% (Takeuchi 2004). These crystals can significantly increase magma viscosity and may impart a yield strength. Consequently, additional dynamic pressure loss occurs. The influence of crystals was not considered in the results shown in **Figures 8** and **9**. At low ascent rates, when timescales for magma ascent are comparable to timescales for crystal growth, the dynamics of magma extrusion may become highly nonlinear and unsteady (Melnik & Sparks 1999). Additional rheological complexities can arise when magmas of different composition (and hence properties) rise simultaneously (Carrigan 2000).

Finally, the location of the fragmentation surface, and the pressure that exists at this boundary, depend on the coupled dynamics of processes in the conduit and the jet at the base of the explosive eruption column.

Despite the simplifications made in our models, they can still be useful for interpreting measurements, and helpful for identifying processes that may be important in a given eruption.

5. NONDIMENSIONAL NUMBERS

Similar to other problems in fluid mechanics, we have seen that dynamics are governed by a set of dimensionless numbers. Some of these and their effects on conduit processes, in particular the Reynolds number, the Peclet number for bubble growth, and the Brinkman number for flow in the conduit, are summarized in **Table 1**. For the most part, inertia can be neglected prior to fragmentation except for low-viscosity mafic magmas. Viscous dissipation can become dynamically important for ascent

Table 1 Dimensionless parameters

Dimensionless number	Process	Value and effect
Re	Bubble growth	$\ll 1$
Re	Magma ascent in conduits	< 1 for silicic magmas prior to fragmentation
Pe_{dif}	Diffusive growth of bubbles	$\gg 1$ for low N_d; supersaturation, and nucleation of new bubbles
Pe_{vis}	Expansion of bubbles	$\gg 1$ if viscosity is high enough; overpressure and fragmentation
Br	Viscous heating near conduit walls	If large enough, lowers viscosity and prevents shear brecciation

rates that characterize the largest silicic eruptions. In addition to these dimensionless numbers, the rheology of magmas is characterized by dimensionless parameters that describe its deformation rate relative to the relaxation time of the melt ($\dot{\epsilon}^*$ in Section 3.4.3) and the relaxation time of bubbles owing to surface tension (capillary number Ca in Section 3.4.5.)

6. CONCLUSIONS AND FUTURE DIRECTIONS

The fluid mechanics of magma ascent in conduits, as shown in **Figure 1**, is conceptually straightforward. Each process that occurs during ascent, e.g., bubble growth, is relatively well understood in isolation of other processes. The material properties that affect magma flow, e.g., rheology and diffusivity, are now routinely measured, even if the measurements themselves are not necessarily routine because of the high temperatures at which measurements need to be made. Thus, it is, in principle, possible to develop models for the fluid mechanics within volcanoes, although the number of processes that often matter make modeling eruptions a formidable problem. Moreover, many of the model parameters that need to be known cannot be measured directly, such as magma supply or conduit geometry and their evolution. The field of modeling eruptions has thus tended to focus on idealized problems in which only certain processes are modeled—the goal being to understand the fluid mechanics of eruptions or to explain a subset of observations, rather than to simulate the entire evolution of a given volcano.

One goal of understanding the fluid mechanics of volcanic eruptions is to provide a systematic physical basis for assessing the hazard posed by volcanoes (**http://volcanoes.usgs.gov**). There are two complementary approaches for assessing hazard. First, the evolution and eruption history of volcanoes are typically determined by interpreting the deposits created by the eruptions. The stratigraphy, texture, and composition of erupted materials provide constraints on the style of eruption that occurred and its temporal evolution. Second, current hazard is assessed by monitoring volcanoes—their deformation, gas release, and seismicity. In both cases the challenge is to relate measurements made outside the volcano to active processes in inaccessible regions far below the surface. Models, such as those reviewed here, provide a starting point for making the needed connections between observations and processes. The picture that has been emerging is that magma ascent rate controls the eruptive

behavior. In turn, flow rate is influenced by magma chamber overpressure, conduit geometry, magma rheology, outgassing, viscous heating, and crystal growth.

ACKNOWLEDGMENTS

M.M. is supported by the National Science Foundation. H.M.G. is supported by a Daly Fellowship. B. Meade and M.O. Saar provided computational resources.

LITERATURE CITED

Alidibirov M. 1994. A model for viscous magma fragmentation during volcanic blasts. *Bull. Volcanol.* 56:459–65

Bagdassarov NS, Dingwell DB. 1992. A rheological investigation of vesicular rhyolite. *J. Volcanol. Geotherm. Res.* 50:307–22

Barmin A, Melnik O, Sparks RSJ. 2002. Periodic behavior in lava dome eruptions. *Earth Planet. Sci. Lett.* 199:173–84

Blackburn EA, Wilson L, Sparks RSJ. 1976. Mechanism and dynamics of strombolian activity. *J. Geol. Soc. London* 132:429–40

Blake S. 1984. Volatile oversaturation during the evolution of silicic magma chambers as an eruption trigger. *J. Geophys. Res.-Solid Earth* 89:8237–44

Blank JG, Stolper EM, Carroll MR. 1993. Solubilities of carbon-dioxide and water in rhyolitic melt at 850-degrees-C and 750 bars. *Earth Planet. Sci. Lett.* 119:27–36

Blower JD, Keating JP, Mader HM, Phillips JC. 2001. Inferring volcanic degassing processes from vesicle size distributions. *Geophys. Res. Lett.* 28:347–50

Boudon G, Villemant B, Komorowski JC, Ildefonse P, Semet MP. 1998. The hydrothermal system at Soufriere Hills volcano, Montserrat (West Indies): characterization and role in the on-going eruption. *Geophys. Res. Lett.* 25:3693–96

Brückner R, Deubener J. 1997. Description and interpretation of the two phase flow behaviour of melts with suspended crystals. *J. Non-Cryst. Solids* 209:283–91

Brückner R, Yue YZ. 1994. Non-Newtonian flow behavior of glass melts as a consequence of viscoelasticity and anisotropic flow. *J. Non-Cryst. Solids* 175:118–28

Büttner R, Zimanowski B. 1998. Physics of thermohydraulic explosions. *Phys. Rev. E* 57:5726–29

Carman PC. 1956. *Flow of Gases Through Porous Media*. San Diego: Academic

Carrigan CR. 2000. Plumbing systems. In *Encyclopedia of Volcanoes*, ed. H Sigurdsson, pp. 219–35. San Diego: Academic

Carrigan CR, Eichelberger JC. 1990. Zoning of magmas by viscosity in volcanic conduits. *Nature* 343:248–51

Cashman KV, Mangan MT. 1994. Physical aspects of magmatic degassing. 2. Constraints on vesiculation processes from textural studies of eruptive products. In *Volatiles in Magmas*, vol. 30 of *Reviews In Mineralogy*, pp. 447–78. Mineral. Soc. Am.

Cashman KV, McConnell SM. 2005. Multiple levels of magma storage during the 1980 summer eruptions of Mount St. Helens, WA. *Bull. Volcanol.* 68:57–75

Costa A. 2005. Viscosity of high crystal content melts: dependence on solid fraction. *Geophys. Res. Lett.* 32:doi:10.1029/2005GL024303
Costa A, Macedonio G. 2002. Nonlinear phenomena in fluids with temperature-dependent viscosity: an hysteresis model for magma flow in conduits. *Geophys. Res. Lett.* 29:doi:10.1029/2001GL014493
Costa A, Macedonio G. 2005. Viscous heating effects in fluids with temperature-dependent viscosity: triggering of secondary flows. *J. Fluid Mech.* 540:21–38
Couch S, Sparks RSJ, Carroll MR. 2003. The kinetics of degassing-induced crystallization at Soufriere Hills volcano, Montserrat. *J. Pet.* 44:1477–502
Denlinger RP, Hoblitt RP. 1999. Cyclic eruptive behavior of silicic volcanoes. *Geology* 27:459–62
Deubener J. 1994. *Thermische und rheologische Eigenschaften hochviskoser und teilkristalliner Lithiumsilicat Schmelzen - Modell für das rheologische Verhalten von Glaskeramiken*. Ph.D. thesis. Technische Universitaet Berlin
Deubener J, Brückner R. 1997. Influence of nucleation and crystallisation on the rheological properties of lithium disilicate melt. *J. Non-Cryst. Solids* 209:96–111
Deubener J, Mueller R, Behrens H, Heide G. 2003. Water and the glass transition temperature of silicate melts. *J. Non-Cryst. Solids* 330:268–73
Dingwell DB. 1996. Volcanic dilemma: flow or blow? *Science* 273:1054–55
Edmonds M, Oppenheimer C, Pyle DM, Herd RA, Thompson G. 2003. SO_2 emissions from Soufriere Hills Volcano and their relationship to conduit permeability, hydrothermal interaction and degassing regime. *J. Volcanol. Geotherm. Res.* 124:23–43
Eichelberger JC. 1995. Silicic volcanism: ascent of viscous magmas from crustal reservoirs. *Annu. Rev. Earth Planet. Sci.* 23:41–63
Eichelberger JC, Carrigan CR, Westrich HR, Price RH. 1986. Non-explosive silicic volcanism. *Nature* 323:598–602
Gardner JE, Denis MH. 2004. Heterogeneous bubble nucleation on Fe-Ti oxide crystals in high-silica rhyolitic melts. *Geochim. Cosmochim. Acta* 68:3587–97
Gardner JE, Hilton M, Carroll MR. 2000. Bubble growth in highly viscous silicate melts during continuous decompression from high pressure. *Geochim. Cosmochim. Acta* 64:1473–83
Gardner JE, Thomas RME, Jaupart C, Tait S. 1996. Fragmentation of magma during plinian volcanic eruptions. *Bull. Volcanol.* 58:144–62
Gerlach TM, Graeber EJ. 1985. Volatile budget of Kilauea Volcano. *Nature* 313:273–77
Giordano D, Dingwell DB. 2003. The kinetic fragility of natural silicate melts. *J. Phys.-Condens. Matter* 15:S945–S54
Gonnermann HM, Manga M. 2003. Explosive volcanism may not be an inevitable consequence of magma fragmentation. *Nature* 426:432–35
Gonnermann HM, Manga M. 2005a. Flow banding in obsidian: a record of evolving textural heterogeneity during magma deformation. *Earth Planet. Sci. Lett.* 236:135–47
Gonnermann HM, Manga M. 2005b. Nonequilibrium magma degassing: results from modeling of the ca.1340 AD eruption of Mono Craters, California. *Earth Planet. Sci. Lett.* 238:1–16

Goto A. 1999. A new model for volcanic earthquake at Unzen Volcano: melt rupture model. *Geophys. Res. Lett*. 26:2541–44
Griffiths RW. 2000. The dynamics of lava flows. *Annu. Rev. Fluid Mech*. 32:477–518
Hammer JE, Cashman KV, Hoblitt RP, Newman S. 1999. Degassing and microlite crystallization in pre-climactic events of the 1991 eruption of Mt. Pinatubo, Phillipines. *Bull. Volcanol.* 60:355–80
Hammer JE, Rutherford MJ. 2002. An experimental study of the kinetics of decompression-induced crystallization in silicic melt. *J. Geophys. Res.-Solid Earth* 107: doi: 10.1029/2001JB000281
Herd RA, Pinkerton H. 1997. Bubble coalescence in basaltic lava: its impact on the evolution of bubble populations. *J. Volcanol. Geotherm. Res*. 75:137–57
Hess KU, Dingwell DB. 1996. Viscosities of hydrous leucogranitic melts: a non-Arrhenian model. *Am. Mineral*. 81:1297–300
Hirth JP, Pound GM, Stpierre GR. 1970. Bubble nucleation. *Metall. Trans*. 1:939–45
Houghton BF, Weaver SD, Wilson CJN, Lanphere MA. 1992. Evolution of a quaternary peralkaline volcano - Mayor-Island, New-Zealand. *J. Volcanol. Geotherm. Res*. 51:217–36
Hurwitz S, Goff F, Janik CJ, Evans WC, Counce DA, et al. 2003. Mixing of magmatic volatiles with groundwater and interaction with basalt on the summit of Kilauea Volcano, Hawaii. *J. Geophys. Res.-Solid Earth* 108: doi:10.1029/2001JB001594
Hurwitz S, Navon O. 1994. Bubble nucleation in rhyolitic melts: experiments at high-pressure, temperature, and water-content. *Earth Planet. Sci. Lett*. 122:267–80
Ichihara M, Rittel D, Sturtevant B. 2002. Fragmentation of a porous viscoelastic material: implications to magma fragmentation. *J. Geophys. Res.* 107:doi: 10.1029/2001JB000591
Jaupart C. 1998. Gas loss from magmas through conduit walls during eruption. In *The Physics of Explosive Volcanic Eruptions*, eds. JS Gilbert, RSJ Sparks, vol. 145, pp. 73–90. London: Geol. Soc.
Jaupart C. 2000. Magma ascent at shallow levels. In *Encyclopedia of Volcanoes*, ed. H Sigurdsson, pp. 237–45. San Diego: Academic
Jaupart C, Allègre CJ. 1991. Gas content, eruption rate and instabilities of eruption regime in silicic volcanoes. *Earth Planet Sci. Lett*. 102:413–29
Jaupart C, Vergniolle S. 1988. Laboratory models of Hawaiian and Strombolian eruptions. *Nature* 331:58–60
Jellinek AM, DePaolo DJ. 2003. A model for the origin of large silicic magma chambers: precursors of caldera-forming eruptions. *Bull. Volcanol*. 65:363–81
Johnson MC, Anderson AT, Rutherford MJ. 1994. Pre-eruptive volatile contents of magmas. In *Volatiles In Magmas*, vol. 30 of *Reviews in Mineralogy*, pp. 281–330. Washington, DC: Mineral. Soc. Am.
Jouniaux L, Bernard ML, Zamora M, Pozzi JP. 2000. Streaming potential in volcanic rocks from Mount Pelee. *J. Geophys. Res.-Solid Earth* 105:8391–401
Kaminski E, Jaupart C. 1997. Expansion and quenching of vesicular magma fragments in Plinian eruptions. *J. Geophys. Res.-Solid Earth* 102:12187–203
Klug C, Cashman KV. 1994. Vesiculation of May 18, 1980, Mount St. Helens magma. *Geology* 22:468–72

Klug C, Cashman KV. 1996. Permeability development in vesiculating magmas: implications for fragmentation. *Bull. Volcanol.* 58:87–100
Knoche R, Dingwell DB, Seifert SA, Webb SL. 1994. Nonlinear properties of supercooled liquids in the Na_2O-SiO_2 system. *Chem. Geol.* 116:1–16
Koyaguchi T. 2005. An analytical study for 1-dimensional steady flow in volcanic conduits. *J. Volcanol. Geotherm. Res.* 143:29–52
Koyaguchi T, Mitani NK. 2005. A theoretical model for fragmentation of viscous bubbly magmas in shock tubes. *J. Geophys. Res.-Solid Earth* 110: doi:10.1029/2004JB003513
Larsen JF, Denis MH, Gardner JE. 2004. Experimental study of bubble coalescence in rhyolitic and phonolitic melts. *Geochim. Cosmochim. Acta* 68:333–44
Lejeune AM, Bottinga Y, Trull TW, Richet P. 1999. Rheology of bubble-bearing magmas. *Earth Planet. Sci. Lett.* 166:71–84
Lejeune AM, Richet P. 1995. Rheology of crystal-bearing silicate melts: an experimental study at high viscosities. *J. Geophys. Res.-Solid Earth* 100:4215–29
Lensky NG, Navon O, Lyakhovsky V. 2004. Bubble growth during decompression of magma: experimental and theoretical investigation. *J. Volcanol. Geotherm. Res.* 129:7–22
Lipman pW, Mullineaux DR, eds. 1981. *The 1980 Eruptions of Mount St. Helens, Washington*, vol. P 1250 of *Professional Paper*. U. S. Geolog. Survey
Liu Y, Zhang YX. 2000. Bubble growth in rhyolitic melt. *Earth Planet. Sci. Lett.* 181:251–64
Liu Y, Zhang YX, Behrens H. 2005. Solubility of H_2O in rhyolitic melts at low pressures and a new empirical model for mixed H_2O-CO_2 solubility in rhyolitic melts. *J. Volcanol. Geotherm. Res.* 143:219–35
Llewellin EW, Manga A. 2005. Bubble suspension rheology and implications for conduit flow. *J. Volcanol. Geotherm. Res.* 143:205–17
Mader HM, Zhang Y, Phillips JC, Sparks RSJ, Sturtevant B, Stolper E. 1994. Experimental simulations of explosive degassing of magma. *Nature* 372:85–88
Manga M, Loewenberg M. 2001. Viscosity of magmas containing highly deformable bubbles. *J. Volcanol. Geotherm. Res.* 105:19–24
Mangan M, Sisson T. 2000. Delayed, disequilibrium degassing in rhyolite magma: decompression experiments and implications for explosive volcanism. *Earth Planet. Sci. Lett.* 183:441–55
Mangan M, Sisson T. 2005. Evolution of melt-vapor surface tension in silicic volcanic systems: experiments with hydrous melts. *J. Geophys. Res.* 110:doi: 10.1029/2004JB003215
Martel C, Dingwell DB, Spieler O, Pichavant M, Wilke M. 2000. Fragmentation of foamed silicic melts: an experimental study. *Earth Planet. Sci. Lett.* 178:47–58
Mason RM, Starostin AB, Melnik O, Sparks RSJ. 2006. From Vulcanian explosions to sustained explosive eruptions: the role of diffusive mass transfer in conduit flow dynamics. *J. Volcanol. Geotherm. Res.* 153:37–50
Massol H, Koyaguchi T. 2005. The effect of magma flow on nucleation of gas bubbles in a volcanic conduit. *J. Volcanol. Geotherm. Res.* 143:69–88
Mastin LG. 2005. The controlling effect of viscous dissipation on magma flow in silicic conduits. *J. Volcanol. Geotherm. Res.* 143:17–28

Mastin LG, Ghiorso MS. 2001. Adiabatic temperature changes of magma-gas mixtures during ascent and eruption. *Contrib. Mineral. Petrol.* 141:307–21

McBirney AR, Murase T. 1970. Factors governing the formation of pyroclastic rocks. *Bull. Volcanol.* 34:372–84

McLeod P, Tait S. 1999. The growth of dykes from magma chambers. *J. Volcanol. Geotherm. Res.* 92:231–46

Melnik O, Sparks RSJ. 1999. Nonlinear dynamics of lava dome extrusion. *Nature* 402:37–41

Melnik O, Sparks RSJ. 2002. Dynamics of magma ascent and lava extrusion at Soufriere Hills Volcano, Montserrat. In *The Eruption of Soufriere Hills Volcano, Montserrat, from 1995 to 1999*, eds. TH Druitt, BP Kokelaar, pp. 153–71. London: Geological Soc.

Mitchell KL. 2005. Coupled conduit flow and shape in explosive volcanic eruptions. *J. Volcanol. Geotherm. Res.* 143:187–203

Mourtada-Bonnefoi CC, Laporte D. 2004. Kinetics of bubble nucleation in a rhyolitic melt: an experimental study of the effect of ascent rate. *Earth Planet. Sci. Lett.* 218:521–37

Mourtada-Bonnefoi CC, Mader HM. 2001. On the development of highly-viscous skins of liquid around bubbles during magmatic degassing. *Geophys. Res. Lett.* 28:1647–50

Mourtada-Bonnefoi CC, Provost A, Albarede F. 1999. Thermochemical dynamics of magma chambers: a simple model. *J. Geophys. Res.-Solid Earth* 104:7103–15

Moynihan CT. 1995. Structural relaxation and the glass transition. *Rev. Mineral. Geochem.* 32:1–19

Mueller S, Melnik O, Spieler O, Scheu B, Dingwell DB. 2005. Permeability and degassing of dome lavas undergoing rapid decompression: an experimental determination. *Bull. Volcanol.* 67:526–38

Namiki A, Manga M. 2005. Response of a bubble bearing viscoelastic fluid to rapid decompression: implications for explosive volcanic eruptions. *Earth Planet. Sci. Lett.* 236:269–84

Navon O, Chekhmir A, Lyakhovsky V. 1998. Bubble growth in highly viscous melts: theory, experiments, and autoexplosivity of dome lavas. *Earth Planet. Sci. Lett.* 160:763–76

Neuberg JW, Tuffen H, Collier L, Green D, Powell T, Dingwell D. 2006. The trigger mechanism of low-frequency earthquakes on montserrat. *J. Volcanol. Geotherm. Res.* In press

Papale P. 1999a. Modeling of the solubility of a two-component $H_2O + CO_2$ fluid in silicate liquids. *Am. Mineral.* 84:477–92

Papale P. 1999b. Strain-induced magma fragmentation in explosive eruptions. *Nature* 397:425–28

Parfitt EA. 2004. A discussion of the mechanisms of explosive basaltic eruptions. *J. Volcanol. Geotherm. Res.* 134:77–107

Parfitt EA, Wilson L. 1999. A Plinian treatment of fallout from Hawaiian lava fountains. *J. Volcanol. Geotherm. Res.* 88:67–75

Polacci M, Rosi M, Landi P, Di Muro A, Papale P. 2005. Novel interpretation for shift between eruptive styles in some volcanoes. *Eos Trans. Am. Geophys. Union* doi:10.1029/2005EO370001
Proussevitch A, Sahagian D, Anderson A. 1993. Dynamics of diffusive bubble growth in magmas: isothermal case. *J. Geophys. Res.* 98:22283–307
Proussevitch AA, Sahagian DL. 1998. Dynamics and energetics of bubble growth in magmas: analytical formulation and numerical modeling. *J. Geophys. Res.-Solid Earth* 103:18223–51
Rosi M, Landi P, Polacci M, Di Muro A, Zandomeneghi D. 2004. Role of conduit shear on ascent of the crystal-rich magma feeding the 800-year-BP Plinian eruption of Quilotoa Volcano (Ecuador). *Bull. Volcanol.* 66:307–21
Rubin AM. 1995. Propagation of magma-filled cracks. *Annu. Rev. Earth Planet. Sci.* 23:287–336
Russell JK, Giordano D, Dingwell DB, Hess KU. 2002. Modelling the non-arrhenian rheology of silicate melts: numerical considerations. *Eur. J. Mineral.* 14:417–27
Rust AC, Cashman KV. 2004. Permeability of vesicular silicic magma: inertial and hysteresis effects. *Earth Planet. Sci. Lett.* 228:93–107
Rust AC, Cashman KV, Wallace PJ. 2004. Magma degassing buffered by vapor flow through brecciated conduit margins. *Geology* 32:349–52
Rust AC, Manga M. 2002. Effects of bubble deformation on the viscosity of dilute suspensions. *J. Non-Newton. Fluid* 104:53–63
Saar MO, Manga M. 1999. Permeability-porosity relationship in vesicular basalts. *Geophys. Res. Lett.* 26:111–14
Saar MO, Manga M, Cashman KV, Fremouw S. 2001. Numerical models of the onset of yield strength in crystal-melt suspensions. *Earth Planet. Sci. Lett.* 187:367–79
Sato H, Fujii T, Nakada S. 1992. Crumbling of dacite dome lava and generation of pyroclastic flows at Unzen volcano. *Nature* 360:664–66
Scandone R, Malone SD. 1985. Magma supply, magma discharge and readjustment of the feeding system of Mount St. Helens during 1980. *J. Volcanol. Geotherm. Res.* 23:239–62
Schmincke HU. 2004. *Volcanism*. Berlin and Heidelberg: Springer
Simmons JH. 1998. Morey Award paper - What is so exciting about non-linear viscous flow in glass, molecular dynamics simulations of brittle fracture and semiconductor-glass quantum composites. *J. Non-Cryst. Solids* 239:1–15
Simmons JH, Mohr RK, Montrose CJ. 1982. Non-Newtonian viscous flow in glass. *J. Appl. Phys.* 53:4075–80
Sparks RSJ. 1978. The dynamics of bubble formation and growth in magmas: a review and analysis. *J. Volcanol. Geotherm. Res.* 3:1–37
Sparks RSJ, Barclay J, Jaupart C, Mader HM, Phillips JC. 1994. Physical aspects of magmatic degassing I. Experimental and theoretical constraints on vesiculation. In *Volatiles in Magmas*, vol. 30 of *Reviews in Mineralogy*, pp. 413–45. Washington, DC: Mineral. Soc. Am.
Sparks RSJ, Huppert HE, Turner JS. 1984. The fluid-dynamics of evolving magma chambers. *Phil. Trans. Roy. Soc. London Ser. A-Math. Phys. Eng. Sci.* 310:511–32
Spieler O, Kennedy B, Kueppers U, Dingwell DB, Scheu B, Taddeucci J. 2004. The fragmentation threshold of pyroclastic rocks. *Earth Planet. Sci. Lett.* 226:139–48

Stasiuk MV, Jaupart C, Sparks RSJ. 1993. On the variations of flow-rate in nonexplosive lava eruptions. *Earth Planet. Sci. Lett.* 114:505–16

Stein DJ, Spera FJ. 2002. Shear viscosity of rhyolite-vapor emulsions at magmatic temperatures by concentric cylinder rheometry. *J. Volcanol. Geotherm. Res.* 113:243–58

Swanson DA, Holcomb RT. 1990. Regularities in growth of the Mount St. Helens dacite dome 1980–1986. In *Lava Flows and Domes: Emplacement Mechanisms and Hazard Implications*, ed. JH Fink, pp. 3–24. Berlin: Springer Verlag

Takeuchi S. 2004. Precursory dike propagation control of viscous magma eruptions. *Geology* 32:1001–4

Takeuchi S, Nakashima S, Tomiya A, Shinohara H. 2005. Experimental constraints on the low gas permeability of vesicular magma during decompression. *Geophys. Res. Lett.* 32: doi:10.1029/2005GL022491

Taylor BE, Eichelberger JC, Westrich HR. 1983. Hydrogen isotopic evidence of rhyolitic magma degassing during shallow intrusion and eruption. *Nature* 306:541–45

Thies M. 2002. *Herstellung und rheologische Eigenschaften von porösen Kalk-Natron-Silicatschmelzen*. Ph.D. thesis. Technische Universitaet Berlin

Thomas N, Jaupart C, Vergniolle S. 1994. On the vesicularity of pumice. *J. Geophys. Res.-Solid Earth* 99:15633–44

Toramaru A. 1989. Vesiculation process and bubble-size distributions in ascending magmas with constant velocities. *J. Geophys. Res.-Solid Earth* 94:17523–42

Toramaru A. 1991. Model of nucleation and growth of crystals in cooling magmas. *Contrib. Mineral. Petrol.* 108:106–17

Toramaru A. 1995. Numerical study of nucleation and growth of bubbles in viscous magmas. *J. Geophys. Res.-Solid Earth* 100:1913–31

Trigila R, Battaglia M, Manga M. 2006. An experimental facility for investigating hydromagmatic eruptions at high-pressure and high-temperature with application to the importance of magma porosity for magma-water interaction. *Bull. Volcanol.* doi:10.1007/s00445-006-0081-6

Tuffen H, Dingwell DB, Pinkerton H. 2003. Repeated fracture and healing of silicic magma generate flow banding and earthquakes? *Geology* 31:1089–92

Vedeneeva EA, Melnik OE, Barmin AA, Sparks RSJ. 2005. Viscous dissipation in explosive volcanic flows. *Geophys. Res. Lett.* 32: doi:10.1029/2004GL020954

Vergniolle S, Jaupart C. 1990. Dynamics of degassing at Kilauea Volcano, Hawaii. *J. Geophys. Res.-Solid* 95:2793–809

Verhoogen J. 1951. Mechanics of ash formation. *Am. J. Sci.* 249:729–39

Villemant B, Boudon G. 1998. Transition from dome-forming to plinian eruptive styles controlled by H_2O and Cl degassing. *Nature* 392:65–69

Voight B, Sparks RSJ, Miller AD, Stewart RC, Hoblitt RP, et al. 1999. Magma flow instability and cyclic activity at Soufriere Hills Volcano, Montserrat, British West Indies. *Science* 283:1138–42

Wallace PJ. 2001. Volcanic SO_2 emissions and the abundance and distribution of exsolved gas in magma bodies. *J. Volcanol. Geotherm. Res.* 108:85–106

Wallace PJ. 2005. Volatiles in subduction zone magmas: concentrations and fluxes based on melt inclusion and volcanic gas data. *J. Volcanol. Geotherm. Res.* 140:217–40

Wallace PJ, Anderson Jr. AT, Davis AM. 1995. Quantification of pre-eruptive exsolved gas contents in silicic magmas. *Nature* 377:612–16

Wallace PJ, Carn SAR, William I, Bluth GJS, Gerlach TM. 2003. Integrating petrologic and remote sensing perspectives on magmatic volatiles and volcanic degassing. *Eos Trans. Am. Geophys. Union* 84:446–47

Webb SL, Dingwell DB. 1990a. Non-Newtonian rheology of igneous melts at high stresses and strain rates: experimental results for rhyolite, andesite, basalt, and nephelinite. *J. Geophys. Res.* 95:15695–701

Webb SL, Dingwell DB. 1990b. The onset of non-Newtonian rheology of silicate melts: a fiber elongation study. *Phys. Chem. Miner.* 17:125–32

Westrich HR, Eichelberger JC. 1994. Gas-transport and bubble collapse in rhyolitic magma: an experimental approach. *Bull. Volcanol.* 56:447–58

Westrich HR, Gerlach TM. 1992. Magmatic gas source for the stratospheric SO_2 cloud from the June 15, 1991, eruption of Mount-Pinatubo. *Geology* 20:867–70

Whitehead JA, Helfrich KR. 1991. Instability of flow with temperature-dependent viscosity: a model of magma dynamics. *J. Geophys. Res.-Solid Earth* 96:4145–55

Wilson L. 1980. Relationships between pressure, volatile content and ejecta velocity in three types of volcanic explosion. *J. Volcanol. Geotherm. Res.* 8:297–313

Wilson L, Sparks RSJ, Walker GPL. 1980. Explosive volcanic-eruptions. 4. The control of magma properties and conduit geometry on eruption column behavior. *Geophys. J. Roy. Astro. Soc.* 63:117–48

Wohletz KH. 1983. Mechanisms of hydrovolcanic pyroclast formation: grain-size, scanning electron-microscopy, and experimental studies. *J. Volcanol. Geotherm. Res.* 17:31–63

Woods AW. 1995. The dynamics of explosive volcanic-eruptions. *Rev. Geophys.* 33:495–530

Woods AW, Koyaguchi T. 1994. Transitions between explosive and effusive eruption of silicic magmas. *Nature* 370:631–45

Wylie JJ, Voight B, Whitehead JA. 1999. Instability of magma flow from volatile-dependent viscosity. *Science* 285:1883–85

Yue YZ, Brückner R. 1994. A new description and interpretation of the flow behavior of glass-forming melts. *J. Non-Cryst. Solids* 180:66–79

Zellmer GF, Sparks RSJ, Hawkesworth CJ, Wiedenbeck M. 2003. Magma emplacement and remobilization timescales beneath Montserrat: Insights from Sr and Ba zonation in plagioclase phenocrysts. *J. Pet.* 44:1413–31

Zhang YX. 1999. A criterion for the fragmentation of bubbly magma based on brittle failure theory. *Nature* 402:648–50

Bird RB, Stewart WE, Lightfoot EN. 1960. *Transport Phenomena*. New York: Wiley. 780 pp.

Lensky ND, Lyakhovsky V, Navon O. 2001. Radial variations of melt viscosity around growing bubbles and gas overpressure in vesiculating magmas. *Earth Planet. Sci. Lett.* 186:1–6

Proussevitch AA, Sahagian DL, Kutolin VA. 1993b. Stability of foams in silicate melts. *J. Volcanol. Geotherm. Res.* 59:161–78

Annual Review of
Fluid Mechanics

Volume 39, 2007

Contents

Indexes

Errata

An online log of corrections to *Annual Review of Fluid Mechanics* chapters (1997 to the present) may be found at http://fluid.annualreviews.org/errata.shtml